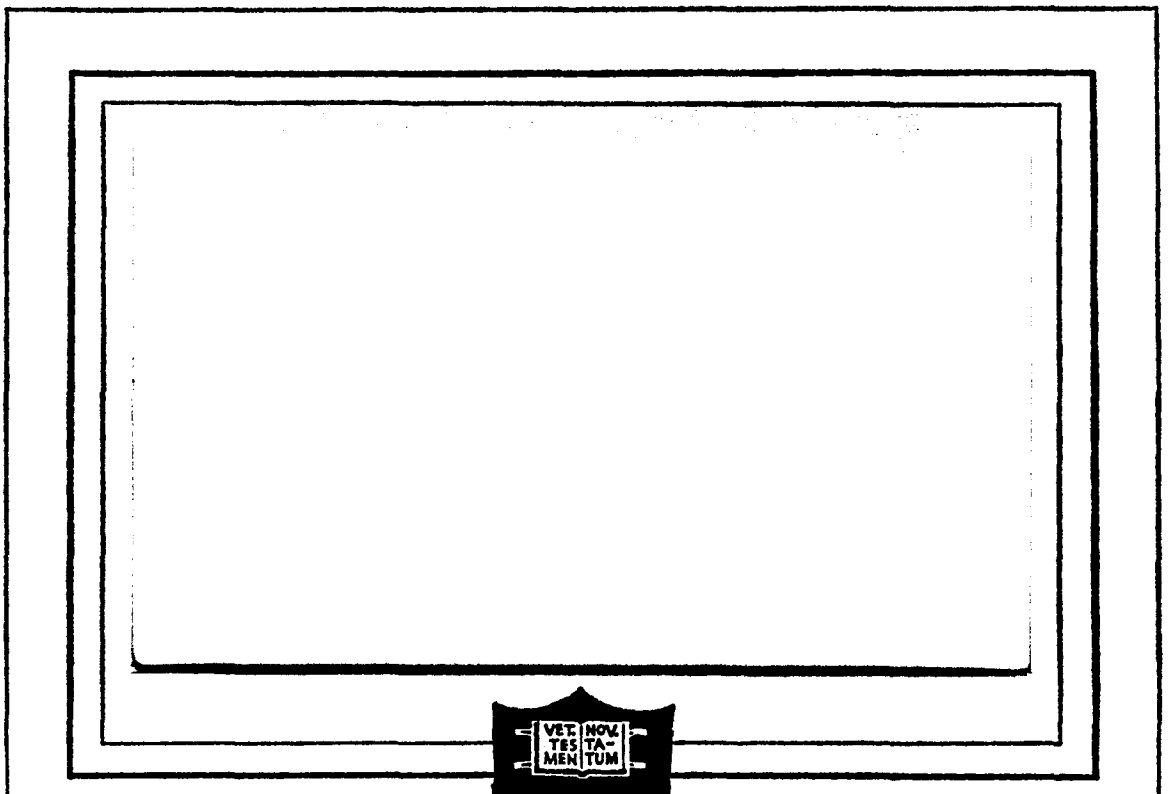

PRINCETON UNIVERSITY

DEPARTMENT OF

AEROSPACE AND MECHANICAL SCIENCES

Fourth Semi-Annual Progress Report
To The

National Aeronautics and Space Administration

On NASA Grant NsG-641

on

PRE-IGNITION AND IGNITION PROCESSES OF METALS

1 November 1965 to 30 April 1966

Report No. 7 8 1

PRINCETON UNIVERSITY

DEPARTMENT OF

AEROSPACE AND MECHANICAL SCIENCES

Fourth Semi-Annual Progress Report
To The

National Aeronautics and Space Administration

On NASA Grant NsG-641

on

PRE-IGNITION AND IGNITION PROCESSES OF METALS

1 November 1965 to 30 April 1966

Report No. 7 8 1

Prepared by: James G. Hansel
James G. Hansel
Research Staff Member

Arthur M. Mellor
Arthur M. Mellor
Assistant-in-Research

Approved by: Irvin Glassman by J.E.H.
Irvin Glassman
Professor
Principal Investigator

1 May 1966

Guggenheim Laboratories for the Aerospace Propulsion Sciences
Department of Aerospace and Mechanical Sciences
PRINCETON UNIVERSITY
Princeton, New Jersey

Fourth Semi-Annual Progress Report
To The

National Aeronautics and Space Administration

On NASA Grant ~~NsG-641~~ NGR-31-001-035
on

PRE-IGNITION AND IGNITION PROCESSES OF METALS

1 November 1965 to 30 April 1966

Report No. 7 8 1

Prepared by: James G. Hansel
James G. Hansel
Research Staff Member

Arthur M. Mellor
Arthur M. Mellor
Assistant-in-Research

Approved by: Irvin Glassman by F.E.H.
Irvin Glassman
Professor
Principal Investigator

1 May 1966

Guggenheim Laboratories for the Aerospace Propulsion Sciences
Department of Aerospace and Mechanical Sciences
PRINCETON UNIVERSITY
Princeton, New Jersey

I. INTRODUCTION

This report is the Fourth Semi-Annual Progress Report to the National Aeronautics and Space Administration by Princeton University on NASA Grant NsG-641, Pre-Ignition and Ignition Processes of Metals, covering the period 1 November 1965 to 30 April 1966.

The second section of the report consists primarily of comments on the general model of heterogeneous ignition presented in the Third Semi-Annual Progress Report. New data from the literature and analytical developments made during the present report period are discussed in Sections III and IV, respectively. In Section V the concluding experiments upon Mo in H_2O mixtures and attempted experiments with Si are described; a discussion of the ignition of Ta and Mo in view of the findings presented in the last Semi-Annual Progress Report is also included.

Most of the experimental emphasis during the present report period, however, was applied to an investigation of the augmentation of Al ignition efficiency by application of surface coatings of Mg and Ca. These experiments were conducted in the wire-burning apparatus and will be described in detail in Section V.

The final section of the report is an outline of future research efforts, which will consist principally of critical and ignition temperature determinations in the newly acquired induction furnace facility.

II. THE PHYSICAL MODEL OF METAL IGNITION

Because the model of heterogeneous ignition has been discussed in detail in the Third Semi-Annual Progress Report, only clarifying comments will be presented here. Much of the present discussion is based on the ignition theory of Frank-Kâmenetskii (1T)[1].

In principle, upon specification of the reactants of interest, the chemical heat release, q_{chem} ($cal/cm^2 sec$), may be calculated as a function of the temperature (T_s) at the interface[2] between the reactants in a heterogeneous system at some specified time, say $t = 0+$.[3] The general result is dis-

---

[1] Numbers in parentheses refer to references listed at the end of the report.

[2] Initially only gas-phase products are considered.

[3] Note that there may be singularities in the reaction rate and conduction heat loss terms at $t = 0$.

played in Fig. 1a. At low temperatures, the dependence is exponential due to the controlling kinetic Arrehenius factor. If the heterogeneous system of interest is a fuel particle in an oxidizing atmosphere, as the surface temperature of the particle increases, diffusion of the oxidizer to the particle surface will become rate-controlling, and the $\dot{q}_{chem}$ curve will have a smaller, but still positive slope, as shown in Fig. 1a. A contribution to the lessening of the slope also results from dissociation of the products.[4]

When the geometry and heat transfer characteristics of the system have been given, it is possible in principle to calculate a heat loss term, $\dot{q}_{loss}$, including conduction into the fuel particle, conduction into the oxidizing gas, and radiation to the surroundings, at t = 0+ and as a function of the interface temperature. In the general model of heterogeneous ignition, the gas-phase products are not allowed to participate in any heat transfer to the environment, in anticipation of the metal ignition case in which the solid-phase products remain stationary on the surface of the fuel particle. (In this latter case, therefore, the entire oxide shell is at the same temperature, namely the temperature of the metal-oxide interface.) The general form of the $\dot{q}_{loss}$ curve is shown in Fig. 1b.

When the $\dot{q}_{chem}$ and $\dot{q}_{loss}$ curves are combined as in Fig. 1c, in general three intersections are possible; these occur at the oxidation (T_{oxid}), critical (T_{crit}), and combustion or flame temperatures (T_f), in order of increasing temperature.[5] These temperatures have been discussed in detail in the Third Semi-Annual Progress Report and represent the only steady-state configurations for the system.

It is possible to envision certain special cases in which only one intersection of the $\dot{q}_{chem}$ and $\dot{q}_{loss}$ curves occurs, and thus only steady-state oxidation or combustion is possible, or in which the curves are tangent (that is, the ignition limit). However, because ignition is of interest here, only the more general case involving a triple intersection (and thus defining a critical temperature) will be considered.

---

[4] Note that the S - shape of the $\dot{q}_{chem}$ curve occurs also in homogeneous gas-phase reactions, but that in this case the leveling at high temperature is due only to dissociation of the products.

[5] Note that the $\dot{q}_{chem}$ and $\dot{q}_{loss}$ curves are similar for both the homogeneous gas-phase case (see Footnote 4), in which the flame temperature is determined by dissociation of the products, and the heterogeneous condensed-phase case, in which T_f is determined not only by dissociation, but also by diffusion of the reactants. The latter then can be generalized to any non-premixed case, including gas-phase diffusion flames. Thus any chemical system may be described by curves of the form shown in Fig. 1.

In the case of metal ignition which is characterized by the formation of a solid-phase product on the metal surface, it is necessary to include in the ignition model the transition temperature (T_{trans}) at and above which the metal-oxidizer system exhibits a linear oxidation rate in ordinary metallurgical experiments. It should be noted that it is not necessary that the film be non-protective above T_{trans} , but rather only that the reaction rate not be inhibited in time as a result of the thickening product film. Furthermore, it is necessary that the rate be linear at all higher temperatures between T_{trans} and T_{ign} .[6]

Two well-known examples of metals which exhibit linear rates at intermediate temperatures but protective (that is, parabolic or cubic) rates at higher temperatures are Al and Be in O_2. Al exhibits a linear rate in O_2 at 500°C (2T) and a protective rate above 660°C(3T). Likewise, the oxidation rate of Be in O_2 is linear between 700 and 750°C (4T) but parabolic between 840 and 970°C (5T). The correspondence between the ignition temperatures of these metals and the respective oxide melting points (6T) suggests that the oxide is generally protective at higher temperatures until it melts and indicates that caution must be excersized in estimating the transition temperature.

The next section of the report consists of a brief review of new experimental data on metal ignition found in the literature survey.

III. THE LITERATURE SURVEY

For convenience, transition temperatures estimated from the oxidation literature are listed in Table 1. All values except that for Zr-O_2 may be taken accurate to ± 50°C. The physical mechanisms responsible for the transition to the linear oxidation rate are discussed in the Third Semi-Annual Progress Report.

The largest amount of new ignition data shown in Tables 2-12 applies to Al in various oxidizing gases (Table 9). All of these data are for non-bulk samples.[7] In general, the

---

[6] T_{ign} , the experimental ignition temperature, is defined as the surface temperature at which the temperature of the metal or the light emitted by the metal begins to increase most rapidly to result in steady-state combustion.

[7] Recall that the critical temperature changes with sample size. Because of the nature of the dust dispersion (DD), quiescent pile (QP), and single particle (SP) experiments, the temperature reported is T_{crit} rather than T_{ign} (see Footnote 6). That is, the initial temperature of the furnace used in these experiments is taken as the ignition temperature. Unfortunately, usually no ignition delay times are given.

values quoted are lower than those for the bulk samples, but the new data (576,577)[8] for Al in CO_2 are considerably higher than those cited previously for non-bulk samples.

In Fig. 2 the variation of ignition (or critical) temperature with surface area to volume ratio is shown for the Zr-air system. The expected trend is observed: as the surface-volume ratio decreases (that is, larger samples), the ignition temperature increases.

Discussion of literature values of ignition temperatures for Ta and Mo will be deferred until Section V.

IV. ANALYTICAL DEVELOPMENTS

The general problem to be solved has been described in detail in Section IV of the Third Semi-Annual Progress Report. Further progress will be described here.

The adiabatic metal problem, in which the oxide film on a spherical metal particle is assumed a perfect thermal insulator, is reduced to solving the equation:

$$\frac{3}{14}B = \frac{\exp\{12.25A\beta^2/9\}}{\sinh\beta}\left[\beta\cosh\beta/2 - 2\sinh\beta/2\right] \qquad (1)$$

for the separation constant β in terms of the non-dimensional input parameters A and B:

$$A \equiv \alpha\rho^2/K_p \qquad (2)$$

$$B \equiv K_p Q/\rho K T_o \qquad (3)$$

where α = fuel thermal diffusivity, cm^2/sec;

ρ = fuel density, g/cm^3;

K_p = parabolic oxidation rate constant, $(g\ metal)^2/cm^4\ sec$;

---

[8]Ignition temperature references are listed at the end of the report.

Q = heat of reaction, cal/g metal;

k = fuel thermal conductivity, cal/cm sec $^{\circ}K$;

T_o = initial temperature of fuel surface, $^{\circ}K$.

Using the definition of α :

$$\alpha = K/\rho c_p \tag{4}$$

where c_p is the fuel specific heat in cal/g$^{\circ}$K, it is seen that

$$B = \frac{1}{A}\frac{Q}{c_p T_o} \equiv \frac{D}{A} \tag{5}$$

Thus Eqn. (1) becomes

$$\frac{3D}{14A} = \frac{\exp\{12.25A\beta^2/9\}}{\sinh\beta}\left[\beta\cosh(\beta/2) - 2\sinh(\beta/2)\right] \tag{6}$$

The initial approach to the solution of this equation had been to attempt to find β for given input A and D , by use of a Newton-Raphson iterative technique based on β . The nature of the numerical results obtained indicated that the computer was seeking the trivial solution $\beta = 0$.

If, however, β and D are given, and a Newton-Raphson iteration for A is used, reasonable results are obtained, because the iteration involves much simpler equations. This technique has been used with success to calculate A as a function of D for the values [9]

$$D = 350;\ 58.3;\ 31.7;\ 21.9;\ 16.6 \tag{7}$$

---

[9] Selected values of input data for the systems of interest are shown in Table 13. Recall that in the case of the binary metal ignition model (that is, Mg on Al in O_2), the metal sphere is considered to be composed of two immiscible metals, one applied as a thin coating on the other. It is assumed that the thermal properties (α , ρ , and k) of the binary system are given by the inner metal which is present in excess, and that the chemical properties (k_p , Q, and T_{trans}) are given by the coating metal, which oxidizes as the temperature increases.

which correspond to the physical cases of interest, and of β over the range 10^{-5} to 10^{4}. The values of A of interest were obtained in the β range 20 to 45 for all of the D given above. The specific values for the cases of interest (clean Al in O_2, Mg on Al in O_2, and Ca on Al in O_2) are shown in Table 13.

The non-dimensionalized temperature, $\theta = T/T_o$, is then calculated from:

$$\theta(\xi,t) = \frac{\sinh\beta\xi}{\xi\sinh\beta}\exp\{\alpha\beta^2 t/r_o^2\} \tag{8}$$

where ξ is the non-dimensionalized radius ($\xi = r/r_o$), r_o is the initial radius in cm, and t is the time in sec. Specializing to the metal-oxide interface temperature, θ_s:

$$\theta_s(\xi_s) = \frac{\sinh\beta\xi_s}{\xi_s\sinh\beta}\exp\{A\beta^2(\frac{1}{\xi_s^2}-\xi_s)^2/9\} \tag{9}$$

For the values of A and β given in Table 13 it was found that θ_s was essentially infinite by the time that the metal-oxide interface had receded to $\xi_s = .9999$. The time required for this regression was for the case of a Mg coating on an Al particle in O_2:

$$t = 1.64\times10^{8} r_o^2 \tag{10}$$

where t is in sec and r_o in cm. In other words, the assumption that the metal is adiabatic has caused an infinite interface temperature rise by the time the surface has regressed .01%.

As a result of this dilemma, a more realistic problem has been solved which includes a heat loss term into the oxide film but not into the surrounding oxidizing gas (the adiabatic particle problem). The following assumptions are made:

(1) All heat addition (that is, the chemical reaction) occurs at the metal-oxide interface. Thus the diffusion of oxidizer through the oxide scale is required for reaction. This assumption is valid in the case of many metal-oxidizer systems.

(2) During the oxidation process, the surface of the metal is smooth, and the entire particle retains spherical symmetry. Thus the temperature is a function only of radius.

(3) All chemical and thermal properties of the metal and oxide are independent of temperature.

(4) Because the thermal conductivity of the surrounding gas is much less than that of the oxide, heat flow across the oxide-gas interface is neglected. Radiation to the surroundings is also neglected.

(5) The oxide shell formed is coherent and continuous; thus the distance the metal-oxide interface has receded can be related to the total particle radius at any time through the Pilling and Bedworth ratio.

By convention, the metallic portion of the particle is denoted by subscript 1 and the oxide portion by subscript 2.

Under the above assumptions the non-steady Fourier heat conduction equation may be written for both regions 1 and 2:

$$\frac{\partial T_i}{\partial t} = \alpha_i \left(\frac{\partial^2 T_i}{\partial r^2} + \frac{2}{r} \frac{\partial T_i}{\partial r} \right) \tag{11}$$

with the initial and boundary conditions (12) - (14) in region 1 and (15)-(17) in region 2:

$$T_1(r_0, 0) = T_0 \tag{12}$$

$$T_1(0, t \neq 0) \neq \infty \tag{13}$$

$$K_1 \left. \frac{\partial T_1}{\partial r} \right|_{r=r_{s-}} = \dot{m}Q - K_2 \left. \frac{\partial T_2}{\partial r} \right|_{r=r_{s+}} \tag{14}$$

$$T_2(r_0, 0) = T_0 \tag{15}$$

$$T_2(r_{s+}, t) = T_1(r_{s-}, t) \tag{16}$$

$$K_2 \left.\frac{\partial T_2}{\partial r}\right|_{r=r_{ox-}} = 0 \tag{17}$$

where T_i = temperature in region i, $^{\circ}K$;

t = time, sec;

α_i = thermal diffusivity of region i, cm^2/sec;

r = radius, cm;

T_o = initial surface temperature, $^{\circ}K$;

r_o = initial particle radius, cm;

k_i = thermal conductivity of region i, cal/cm sec $^{\circ}K$;

$\left.\frac{\partial T_1}{\partial r}\right|_{r=r_{s-}}, \left.\frac{\partial T_2}{\partial r}\right|_{r=r_{s+}}$ = temperature gradients at r_s into the metal and oxide, $^{\circ}K/cm$;

$\dot{m}$ = reaction rate, g metal/cm^2sec;

Q = chemical heat release, cal/ g metal;

$\left.\frac{\partial T_2}{\partial r}\right|_{r=r_{ox-}}$ = temperature gradient at r_{ox} into the oxide, $^{\circ}K/cm$;

r_s = radius of metal-oxide interface, cm;

r_{ox} = total particle radius, cm.

Non-dimensionalization is accomplished as follows:

$$\theta_i \equiv T_i / T_0 \tag{18}$$

$$\xi \equiv r / r_0 \tag{19}$$

$$\tau_i \equiv \alpha_i t / r_0^2 \tag{20}$$

Eqns. (11) through (17) then become:

$$\frac{\partial \theta_i}{\partial \tau_i} = \frac{\partial^2 \theta_i}{\partial \xi^2} + \frac{2}{\xi} \frac{\partial \theta_i}{\partial \xi} \tag{21}$$

$$\theta_1(1,0) = 1 \tag{22}$$

$$\theta_1(0, \tau \neq \alpha) \neq \alpha \tag{23}$$

$$K_1 \left.\frac{\partial \theta_1}{\partial \xi}\right|_{\xi=\xi_{s-}} = \frac{r_0 \dot{m} Q}{T_0} - K_2 \left.\frac{\partial \theta_2}{\partial \xi}\right|_{\xi=\xi_{s+}} \tag{24}$$

$$\theta_2(1,0) = 1 \tag{25}$$

$$\theta_2(\xi_{s+}, t) = \theta_1(\xi_{s-}, t) \tag{26}$$

$$K_2 \left.\frac{\partial \theta_2}{\partial \xi}\right|_{\xi=\xi_{ox}} = 0 \tag{27}$$

The general solution of Eqn.(21) is :

$$\theta_i = \frac{1}{\xi}\left\{C_{2i}\sinh\beta_i\xi + C_{3i}\cosh\beta_i\xi\right\}\exp\left\{\beta_i^2\tau_i\right\} \tag{28}$$

where C_{2i}, C_{3i}, and β_i are constants. Applying Eqns. (22) and (23):

$$C_{31} = 0 \tag{29}$$

$$C_{21} = 1/\sinh\beta_1 \tag{30}$$

Thus:

$$\theta_1 = \frac{\sinh\beta_1\xi}{\xi\sinh\beta_1}\exp\left\{\beta_1^2\tau_1\right\} \tag{31}$$

as in the adiabatic metal problem. There are now four equations, Eqns. (24)-(27), in four unknowns, C_{22}, C_{32}, β_1, and β_2. The former two may be eliminated through Eqns. (25) and (27) to give:

$$\theta_2 = \frac{1}{A_4\xi}\left\{A_2\sinh\beta_2\xi + A_1\cosh\beta_2\xi\right\}\exp\left\{\beta_2^2\tau_2\right\} \tag{32}$$

where

$$A_1 \equiv \beta_2\cosh\beta_2\xi_{ox} - \frac{1}{\xi_{ox}}\sinh\beta_2\xi_{ox} \tag{33}$$

$$A_2 \equiv \frac{1}{\xi_{ox}} \cosh\beta_2 \xi_{ox} - \beta_2 \sinh\beta_2 \xi_{ox} \tag{34}$$

$$A_4 \equiv A_1 \cosh\beta_2 + A_2 \sinh\beta_2 \tag{35}$$

β_1 and β_2 are the remaining unknowns which may be obtained from the the solution of Eqns. (24) and (26), where:

$$\dot{m} = 3K_p / 2\rho_1 r_0 \left(\frac{1}{\xi_s^2} - \xi_s\right) \tag{36}$$

$$t_s = \rho_1^2 r_0^2 \left(\frac{1}{\xi_s^2} - \xi_s\right)^2 / 9K_p \tag{37}$$

$$\gamma_i = \alpha_i t / r_0^2 \tag{38}$$

$$\gamma_{is} = \alpha_i \rho_1^2 \left(\frac{1}{\xi_s^2} - \xi_s\right)^2 / 9K_p \tag{39}$$

$$\xi_{ox} = \sqrt[3]{\xi_s^3 + \gamma(1 - \xi_s^3)} \tag{40}$$

where ρ_1 is the metal density in g/cm^3. ξ_s is taken as 0.5 in Eqns. (24) and (26) because $\dot{m}$ (Eqn. (36)) is infinite at $\xi_s = 1$. The non-dimensional input parameters are defined as:

$$B_i \equiv \alpha_i \rho_1^2 / K_p \tag{41}$$

$$B_3 \equiv Q / c_{p_1} T_0 \tag{42}$$

The selected input values are shown in Table 14 for cases of interest. The problem was solved by use of a brute force method to search for the approximate solutions β_{10} and β_{20}, which were then used as the initial values in a two-dimensional Newton-Raphson iterative technique based on β_1 and β_2. The results are shown in Table 14 for the physical cases of clean Al in O_2, Mg on Al in O_2, and Ca on Al in O_2.

Temperature calculations from Eqn. (31) are currently in progress.

The next section of the report consists of a discussion of experimental progress made during the report period. In particular, Mo-H_2O reactions and Si experiments are reported, the ignition of Ta and Mo is discussed, and an investigation of the ignition of Al wires coated with thin films of Mg and Ca is reviewed.

V. EXPERIMENTAL RESULTS

1. Molybdenum in H_2O Mixtures

An investigation of the ignition and combustion of Mo in pure H_2O at 50 and 100 torr (1 torr = 1 mm Hg) and in 50%-50% mixtures of H_2O-O_2, H_2O-Ar, and H_2O-CO_2 at 50, 100, and 200 torr was carried out in order to complete the investigation of Mo in the wire-burning apparatus. The sample specifications and reaction mechanisms have been described in detail in the Third Semi-Annual Progress Report. The averaged data for Mo are presented in Table 15.

In H_2O-O_2 mixtures at all pressures the white, solid-phase combustion, previously denoted as regime one, was observed. In pure H_2O and H_2O-Ar mixtures the simple melting mechanism previously observed in pure Ar (regime two) occurred, and in H_2O-CO_2 mixtures both regimes two and four were found, the latter occurring more consistantly at the higher pressures.

Recall that in a similar investigation of the ignition and combustion of Ta wires it was found that the solid-phase combustion mechanism of Ta in O_2 was impeded by CO_2 and accelerated by H_2O. In the case of Mo, however, no similar effect was found, as neither H_2O nor CO_2 as the diluent in 50% O_2- 50% diluent mixtures impeded the solid-phase combustion observed in pure O_2.

In the Third Semi-Annual Progress Report, a sub-oxide, vapor-phase diffusion flame observed by Bartlett (12T) was discussed. Attempts to duplicate this phenomenon in the present apparatus by changing the voltage rise rate from about .117 to .235 v/sec were unsuccessful. However, Bartlett used a commercial welding DC power supply with 800 amps maximum current output and with manual control to ignite his samples (13T). Since the rating of our ignition apparatus is 100 amps at 24 VAC, it is not unexpected that the sub-oxide diffusion flame could not be reproduced.

2. The Ignition of Tantalum and Molybdenum[10]

Applying the ignition criterion to Ta and Mo, the transition temperatures for Ta in O_2 may be taken as about 500°C and 700°C respectively (Table 1). The physical mechanisms responsible for the transition to the linear oxidation rate are mechanical stress cracking (type [f]) for Ta and perhaps also for Mo, although vaporization of the oxide MoO_3 is important in the latter case (type [b]). No critical temperature estimates have been found for either metal; however, Albrecht et al. (14T) report an ignition delay time of 15 min at 1250°C for Ta in O_2 at 1 atm.

Reported ignition temperatures for Ta and Mo are summarized in Tables 6 and 7. Except for the QP results, in which self-heating is usually an important factor,[11] all ignition temperatures are above the corresponding transition temperatures. In the case of Ta, the large discrepancy between the transition and ignition temperatures indicates that the critical temperature may be controlling (as the results of Albrecht et al. (14T) would suggest).

Recall that in the present investigation a high temperature, non-self-sustained oxidation reaction was observed with Ta (regime two). Large macrocracks were observed on the wire surface, and the wire glowed with a dull orange-red heat. Both of these observations indicate that the wire temperature had exceeded the transition temperature. However, because the reaction was not self-sustaining at this point, by definition it was not occurring above the critical temperature. Thus for this experiment as well as for that of Albrecht et al. (14T), the critical temperature of Ta apparently exceeds its transition temperature and thus controls its ignition temperature.

In the case of Mo, that ignition occurs after the oxide melts is consistent with the results of other investigators (see Table 7) and with the ignition criterion. As stated previously, the proximity of the transition and ignition temperatures of Mo in O_2 suggests that the former temperature, rather than the critical

---

[10] During the report period a paper entitled "Combustion Reactions of the Refractory Metals Tantalum and Molybdenum" has been written by A. M. Mellor and I. Glassman. The paper was given at the 1966 Spring Meeting of the Western States Section, The Combustion Institute, and has been submitted for publication in the Journal of the Electrochemical Society.

[11] That is, because of the large surface area available for reaction, but the small surface area available for heat loss to the surroundings, T_{crit} will be especially low for this configuration.

temperature, controls the ignition process. No conclusions to the contrary could be reached on the basis of the present investigation.

To summarize, the ignition of Ta in O_2 is controlled by the critical temperature (as for Mg in air or O_2), whereas that of Mo in O_2 is controlled by the transition temperature (as for Al in O_2)

3. Silicon

Initial experimentation was carried out with pure Si rods 11 cm long and 6.3 mm in diameter. Due to the high resistivity of pure Si, no current flowed through the samples as the voltage across them was increased. P doped, n-type Si rods of the same dimensions were then used. Both types of specimens were supplied by the Chemical Materials Department of Texas Instruments Inc.

The n-type Si could be heated in O_2 to a dull red glow with an expenditure of somewhat less than the 2000 watts obtainable from the power supply. At this point the rod generally broke near the electrode blocks (i.e., in a region of extremely large thermal gradients) with subsequent arcing, or merely stopped conducting any current greater than 1 amp. The latter phenomenon is attributed to loss of the P at high temperatures. In either case, little of any reaction was found to have occurred on the surface of the rod. Because of the extreme brittleness of the samples, their cross section could not be lessened in a small length of the rod to provide a local hot spot. At this point further experimentation with Si was discontinued.

4. Augmented Aluminum Ignition Efficiency

To reiterate briefly, it is the high transition temperature of Al (or Be) which may lead to deviations from theoretical performance in solid propellant rocket systems. Application of thin coatings of Mg or Ca on an Al particle should alleviate this difficulty as these metals are characterized by low transition temperatures. Analytical developments to calculate the necessary coating thickness have been described in Section IV. An experimental investigation of the ignition of Al wires coated with Mg or Ca, performed in the wire-burning apparatus during the report period, will now be described.

a. Experimental Apparatus and Procedure:

Thin coatings of Mg and Ca have been applied to Al wires by means of vacuum deposition; the resulting samples were then burned in the wire-burning apparatus in pure O_2 at pressures of 50 , 100, 300, and 500 torr and 1, 2, and 5 atm. The most significant data are the values of total power at breaking (which include

factors due to the electrodes, etc.) for the variously treated samples. Above 100 torr of O_2, breaking occurs at the melting point of Al_2O_3 (2030°C) for the ordinary samples; at 50 and 100 torr the thermal Al_2O_3 coat is unable to support the Al, which melts at 660°C. In O_2, ignition occurs at the melting point of the oxide, within 5 msec of the wire's breaking, which is the resolution attainable from the detection apparatus. Thus, if any effect of the coating material is felt, the total power at breaking should be different from that of the ordinary Al wires.

Data for Al wires in Ar represent a lower limiting case for the experiment; here only the 50 Å room-temperature Al_2O_3 coat is present on the Al wire surface, and there is almost no structural support available for the wire from the oxide. When the Al melts, the wire will break almost immediately. Thus if the coating metal were fulfilling its purpose it would oxidize preferentially during the heating period (as well as during storage) and prevent any formation of Al_2O_3. Any structural strength would result from the presence of the coating metal and coating metal oxide, and in the limit, for an effective coating, the power required to break the coated wire in O_2 would approach that required to break the Al wire in Ar. Thus, the only significant result which is obtainable in the wire-burning apparatus (in which the sample must support itself during the heating period) which indicates the effectiveness of the coating in preventing Al_2O_3 formation is that the power at breaking in O_2 for the coated wire be as close as possible to the power at (essentially) melting for the Al wire in Ar.

All Al wires were 11 cm long and of 0.89 mm diameter. They were the standard Al used in previous investigations in this laboratory, Reagent No. A-557, Fisher Scientific Co. with major impurities Ca, Cu, and Na. The Ca was supplied by A. D. MacKay, Inc. in the form of 0.76 mm sheet. It was then sheared into approximately 2 cm long pieces with square cross section for vacuum coating; its purity was 99.0% with the balance largely $CaCl_2$, according to the supplier. 99.9%+ Mg rod of 3.18 mm diameter was obtained from the same supplier and was cut into about 2 cm long pieces. Approximately 350 mg of either coating material was used as a coating dose.

All vacuum deposition was performed in a Consolidated Vacuum Corporation Model LCl-14B Laboratory Vacuum System, at pressures on the order of 5×10^{-5} torr. The coating material was held in tantalum boats with tantalum wire. Generally, during the coating process the potential drop across the Ta boat was maintained constant, with occasional flashing. Several static geometric orientations of the Al wires with respect to the Ta boat were used, and in all cases patchy deposits were obtained. Weight gains for the individual wires were irreproducible. Batches included anywhere from 5 to 16 Al wires, and up to 3 coating doses were employed for the individual batches.

A motor was then inserted into the bell jar of the coating apparatus and 16 wires were mounted horizontally in a squirrel cage arrangement around the rotating shaft, 8 to 10 cm above the Ta boat. In this configuration about 9 cm of each wire was coated. The motor speed was measured to be 3650 rpm in air at one atm. Upon application of this technique, extremely reproducible weight gains were attained on the individual wires within any given batch. Also, to the naked eye the coating deposits were much more uniform than those obtained previously.

Four substrate preparations previous to vacuum deposition were used (see Table 16). The first Al wire pretreatment was a short ($\sim$ 5 min) wash in Benzin at 25°C followed by a one hour or less degassing period; this wire after pretreatment is referred to as AL1 (the as-received wire with no pretreatment is called AL). The second pretreatment consisted of a 30 min wash in methanol at 25°C followed by one hour of degassing[12] (AL2). Obviously neither the AL1 or AL2 pretreatment removed the pre-existing, room temperature Al_2O_3 film from the Al substrate.

In the third and fourth pretreatments the oxide was removed from the substrate. The pretreatment used for the AL3 wires consisted of a 2 min immersion in a $HgCl_2$ solution followed by a 15 min wash in CH_3OH. The wires were subsequently wiped to remove the remaining sludge on their surfaces and to reveal a bright and shiny substrate. No effort was made to investigate the effect of the strength of the $HgCl_2$ solution. A fresh saturated solution (6.9g $HgCl_2$ per 100 ml dist. H_2O at 25°C) was used approximately every 8 batches (i.e., every 128 wires[13]). The general appearance of the wires after pretreatment was similar irrespective of the strength of the solution.

A one hour etch in a dilute HF solution followed by a 15 min rinse in methanol formed the AL4 pretreatment. The acid solution was initially 2% HF and was changed every 8 batches (128 wires); the methanol was changed every 4 batches (64 wires).

The AL1 and AL2 wires were tagged and weighed indivi-

---

[12] If the wires were not outgassed, erratic results were obtained during their initial weighings due to evaporation of the Benzin or methanol.

[13] Throughout, one batch equals 16 Al wires. Each individual coating process is referred to as a dose, that is, three doses of Mg refers to three coating operations, each of which started with 350 mg of Mg.

dually before and after coating. Examples of the excellent individual weight gain reproducibilities from wire to wire within a batch obtainable in the squirrel cage coating assembly are shown in Table 17.[14] The AL1 and AL2 wires were exposed to air at all times before and after coating.

The AL1 pretreatment was discontinued for two reasons: firstly, in attempting to ignite AL1 wires with no coating present, occasionally sparks were observed in the gas phase near the sample before the sample began to glow brightly (possibly gas-phase ignition of the Benzin remaining after the pretreatment); secondly, large flakes of Ca spalled off the Al wires which had been pretreated with Benzin. Neither of these difficulties were observed with the AL2 (methanol washed) wire, although a much smaller amount of Ca did spall off even in this case. It is important to note that the gas-phase sparking phenomenon was not observed with as-received Al wire (AL wire) either when burned during this report period or when burned in all previous investigations in this laboratory.

The pretreatments in which the Al_2O_3 films were removed were carried out in the Vacuum/Atmospheres Corporation Dri-Train purchased under the subject contract. The Dri-Train was filled with Ar. After pretreatment all 16 wires were placed in a weighing tube of known weight and removed from the Dri-Train; the assembly was then weighed and returned to the Dri-Train. Thus the weighing tube was filled with Ar at all times except for a brief interval while re-entering the Dri-Train, i.e., during evacuation of the antechamber of the Dri-Train, at which time the rubber stopper popped from the weighing tube. Subsequent examination of the AL3 wires indicated that 2 to 3 cm of the wires closest to the mouth of the weighing tube had suffered some oxidation during the exposure to air in the depressurizing antechamber. The resulting film was not removed.

After the wires had been returned to the Dri-Train, they were placed in the squirrel cage arrangement used in the AL1 and AL2 investigations. Within the Dri-Train, the entire squirrel cage arrangement was placed in a large airtight plexiglass tube (which was thus filled with Ar) and stoppered. This assembly was removed from the Dri-Train, transported to and installed in the coating bell jar. The coating jar was then evacuated. At low pressure the plexiglass covering tube was opened by means of

[14] Calculation of the weight of a uniform coating of thickness 1 μ distributed along 9 cm of an 0.89 mm wire gives .875 and .779 mg for Mg and Ca respectively, where the respective densities have been assumed to be 1.74 and 1.55 (7T). Thus for the batches shown in Table 17 the Ca coating thickness is on the order of 1 μ, and that of Mg 2/3 μ.

a pulley arrangement to expose the samples for coating as is shown in Fig. 3. (The bell jar has been removed for the purposes of these photographs. The Ta boat containing the coating metal is indicated with an arrow in the lower photograph.) Coating was then accomplished as usual. If more than one dose was to be applied to the batch, the bell jar was filled with Ar and the covering tube replaced before the bell jar was opened to the atmosphere.

After the coating operation had been completed, the wires were removed from the squirrel cage and weighed in the original weighing tube. They were then stored in the laboratory until use since the presence of an oxide on the coating metal is permissable. In summary, note that the only exposure of the wires to air after pretreatment and before completion of the coating was during reentry into the Dri-Train after the initial weighing. This exposure, however, is thought to affect only a small length of the wires.

Averaging the weight over the 16 wires in the batch before and after coating is felt to be accurate because of the excellent reproducibility of weight gain from wire to wire observed for the AL2 wires coated in the squirrel cage arrangement. (See in particular Table 17.)

For the AL2 wires, the average weight gain per wire from batch to batch was extremely reproducible, as is shown in Table 18. The nomenclature used is as follows: AL2MG2 represents samples of AL2 given two doses of Mg, AL2CA1 represents samples of AL2 given one dose of Ca, etc. Unless otherwise indicated, all batches were tested in the wire-burning apparatus one day after coating was accomplished.

For the AL3 and AL4 wires, the reproducibility from batch to batch,however, was not as good (Tables 19 and 20). This effect is thought to result from either the outgassing of the CH_3OH between weighings or the spalling of the Al_2O_3 whiskers, characteristic of amalgamated Al, which formed at the uncoated ends in the case of the AL3 wires. Similarly, the former effect most likely causes the discrepancies between the AL4 batches. In any case, it is assumed that coatings commeasurate with the AL2 coatings (that is, 1 to 3 μ) were obtained with the AL3 and AL4 wires. The data from the various similarly treated batches used in the power averages did not in general show wide differences.

b. Storability of the Treated Wires:

Aging of the coatings is of interest if the propellant-additive formulation is to be storable. For this reason one of each of the various types of batches were observed for a week before testing in the wire-burning apparatus. The weights presented

in Tables 21-23 are averaged over the 16 wires of each batch; the balance accuracy is ± 0.1 mg. Between the fourth and seventh day weighings the batches were outgassed for 65.5 hr.

From Table 21 it is seen that there is no essential change in the average weights of the AL2MG1, AL2MG2, and AL2MG3 batches (numbers 23, 40, and 39) over the week, nor was any physical change in the wires seen with the naked eye. Note in particular that 65.5 hr of outgassing had no effect on the weight. Thus it is concluded that AL2MG wires are storable.[15]

The AL2CA batches (numbers 23, 38, and 37) do not have this property, however: the average weight increased after 1 day and decreased after the outgassing. Furthermore the coatings, which were originally a yellowish black, were observed to have changed color after 1 day. At this time the coating was very close to the shiny metallic color of the Al wire and could be distinguished from the substrate only with difficulty. Since the batch lost weight after the outgassing some of the weight gain and color change is attributed to a Ca gettering action. The remainder of the weight gain is attributed to oxidation of the Ca, and the erratic weight losses are attributed to spalling of the Ca or CaO from the wire. Thus the AL2CA wires are not storable.

In general, the AL3 coatings exhibit the same behavior, as is shown in Table 22. All the weight losses for the AL3MG coatings were a result of spalling of the Al_2O_3 whiskers which formed at the uncoated wire ends due to the amalgamation pretreatment. Only occasionally was a whisker observed to penetrate the coated area of a wire, and it is concluded that AL3MG wires are storable.

Amalgamation of the substrate increased the spalling of the Ca, and AL3CA wires are less storable than AL2CA wires.

The HF etch pretreatment (AL4) was expected to increase the degree of surface roughness of the Al substrate, which has two effects: a better mechanical bond between the coating and substrate was expected, and the probability of pinholes in the coating was expected to increase. The constant nature of the averaged weights for both the AL4MG and AL4CA wires, shown in Table 23, substantiates the former expectation. The weight gains for the AL4CA wires between the zeroth and first day weighings is again attributed to adsorption by and/or oxidation of the Ca coatings.

[15] Storable as used here and elsewhere in this report is understood to involve times up to one week.

However, both types of AL4 wires are apparently storable.

Batch 79 was treated with a fresh HF solution, and the remaining batches shown in Table 23 were treated in chronological order in the same solution. Since the average initial weight of the Al wires used was typically 185.0 mg, it is seen that about 15 mg of Al was removed upon the sixth use of the HF solution (batch number 84). It is thus concluded that some etching was accomplished in all cases with the HF solutions, even after seven uses (recall that the etching solution was replaced every eight batches).

c. Visual Observations in the Wire-Burning Apparatus:

For the Mg coated wires (that is, AL2MG, AL3MG, and AL4MG wires), during the ohmic heating period in the wire-burning apparatus gas-phase sparks were observed near the wire as it approached a dull-red heat. Their reproducibility is indicated in Tables 24-26, along with the ignition reproducibility for the various wires. Note that sparks were not observed with the AL (as-received Al), AL2, AL3, or AL4 wires. Thus the sparks observed with the Mg coated wires are thought to be the Mg in the coating igniting in the vapor phase. The Mg ignition temperature in O_2 is about 630°C, which is consistent with the dull red heat of the wire. In general, the frequency, size, and brightness of the sparks increased as the number of coating doses increased.

As the Ca coated wires were heated to a dull glow, thin transparent flakes of several mm^2 area were noted to peel off of the wire. Only on rare occasions were gas-phase sparks observed (see Tables 24-26). Evidently, then, the Ca is consumed through solid-phase oxidation during storage or as the wire is heated (note that sparks were observed on 12 out 14 experiments with AL2CA1 wire tested immediately after coating (Table 24)).

Whenever ignition occurred for any of the variously treated wires (AL through AL4CA), a brilliant blue-white flame regressed to the electrode blocks and was quenched. The combustion duration was on the order of ½ sec. The products consisted of grey metallic spheres and white smoke. Occasionally, combustion continued at the electrode blocks for one or two sec; in this case white-grey glassy spheres were also found (in earlier work similar spheres were identified as $\alpha - Al_2O_3$). The diameter of both metal and oxide spheres was several mm.

Because at least visually the combustion and products of combustion were equivalent to those observed previously in this laboratory with Al wires in O_2, it is concluded that the pretreatments and coatings affected only the Al ignition, but not combustion.

d. Effect of the Coatings upon Ignition:

Average total power at breaking for AL2MG wires versus total O_2 pressure is shown in Fig. 4. A logarithmic abscissa is used to separate the data points. Data points for as-received Al (AL), AL2, and AL wires in Ar are also shown. Recall that for an effective coating, the average total power at breaking should fall between that for the AL or AL2 wires and that for Al in Ar. With the exception of the one week old data, each data point represents the averaged value of total power at breaking at a given pressure for at least two experiments in which wires from different batches were used. Recall that unless otherwise noted, all batches were tested one day after coating.

Recall that below 300 torr (5.92 psia) the normal wires do not break at the melting point of Al_2O_3, but rather near the melting point of Al, as little oxide is formed during the heating period to support the molten Al. Thus, characteristically, powers are lower below this pressure. This observation is consistent with the fact that the wires attained only red heat below and white heat above this pressure. The general trend to higher powers at higher pressures is due to both increasing convective losses and increasing oxide thicknesses (i.e., there is more oxide to melt) due to higher reaction rates with increasing O_2 pressure.

The very significant trend apparent from Figure 4 is that the total power at breaking for Mg coatings (1,2, or 3 doses) is greater than that for the as-received or AL2 wires (which are essentially equivalent).

The increase in total power at breaking for the wires coated with Mg is attributed to the presence of a MgO film, which is most likely formed as the wire is heated. (Recall that the Mg coated wires do not change in weight or in color during a one week period after coating.) The Mg vaporizes and ignites in the gas phase adjacent to the wire. Since the MgO is above its transition temperature, the Al will continue to oxidize. When the wire breaks, either the power is higher because of the added MgO film which acts as a heat sink, or the molten Al_2O_3 seals the porous MgO film, which is then able to support the wire until the MgO sublimes at 2770°C(11T). A third possibility is the formation of an Al_2O_3-MgO alloy which one would expect to have a melting point above that of Al_2O_3 but below that of MgO. In any case, the effect is contrary to the desired result.

The coincidence of the one day old and one week old data points substantiates the conclusion that the AL2MG wires are storable.

Fig. 5 shows the total power versus total pressure for the various AL2CA wires as well as for AL, AL2 and AL in Ar wires. In general, the powers required to break the one day old AL2CA1, AL2CA2, and AL2CA3 wires falls between that for the AL (or AL2) wires and that for the AL in Ar wires. This effect is attributed to the ability of the Ca (or CaO) coating to inhibit somewhat the Al oxidation during the heating process, in spite of the visible spalling of the coating. As can be seen from Table 24, essentially no gas-phase sparks were observed as the one day old and one week old wires were heated, whereas with AL2CA1 wires tested immediately after coating, sparks were observed on 12 out of 14 runs.

It is thus concluded that even after one day most of the Ca coating has oxidized to CaO (or has done so before it reaches its ignition temperature during the ohmic heating period), because only the fresh batches exhibited the sparks. Some of the CaO spalled from the wire during storage, but that which remained was sufficient to inhibit the Al oxidation during the heating process to the point that the power required to break these samples was less than that for the AL and AL2 wires. A second explanation of the lower power requirement is that the remaining Ca or CaO combines with the pre-existing Al_2O_3 coat in such a way as to lower its transition temperature. Because no temperature estimates are available from the wire-burning apparatus, and because of undertainties in the value of the Al critical temperature, it is difficult to exclude either mechanism postulated above, although the former is felt more likely.

It is seen in Fig. 5 that the one week old samples exhibit considerable scatter and in general do not agree well with the one day old wires. This fact most likely results from the randomness of the spalling on the individual wires and further indicates that the AL2CA wires are not storable even for times as short as a week.

Averaged data are shown in Fig. 6 for the AL3MG, AL, AL3, Fresh AL3, and AL in Ar samples. One notes immediately that the one day old AL3 samples require higher powers than do the AL samples, which is explained by the thick, self-healed Al_2O_3 film which had formed on the former wires after one day in air. It was not expected, of course, that the amalgamated AL3 wires should be storable. The fresh AL3 results, for which the wires were exposed to air only as the wire-burning apparatus was evacuated, are in general somewhat lower than the AL results. The 100% incidence of ignitions shown in Table 25 indicates that in all cases for the fresh and one day old AL3 wires the critical temperature was attained before the wire broke, even at the lower O_2 pressures. The thick Al_2O_3 film supported the molten Al until T_{crit} was exceeded at all O_2 pressures.

The AL3MG results in Fig. 6 show the desired result and indicate that a 1 to 3 μ Mg coating is capable of preventing Al_2O_3 formation during one week storage in air at 25°C and during the ohmic heating period, even when the substrate has been amalgamated. These coatings appeared the same as those on the AL2 substrate, and only occasionally was an Al_2O_3 whisker observed to have penetrated the coat, except near the uncoated ends. The conclusion is thus reached that it is extremely desirable to remove the pre-existing Al_2O_3 film before coating Al with Mg in order to improve the Al ignition in O_2.

Note that at 5 atm all the coatings have approached the power required to break the AL wire. This fact may indicate that thicker coatings are required at higher O_2 pressures.

Similar data are presented for the AL3CA wires in Fig. 7. It is seen that the AL3CA1 and AL3CA3 wires were unable to prevent Al oxidation, which is not unexpected, due to the spalling of the coating on AL2 substrates (the amalgamation increased this effect). On the other hand, the AL3CA2 samples show the desired trend for no apparent reason.

Total power at breaking for the AL4MG wires is shown in Fig. 8. It is seen that the AL4 and fresh AL4 results are quite similar. The one day old AL4MG1 and AL4MG2 data exceed those for the uncoated wire, whereas the AL4MG3 data are somewhat better and the AL4MG4 data are considerably better than those for the etched, but not coated wire.

It was initially felt that after the wire was etched, some oxidation was occurring on its surface, either during storage in the Dri-Train prior to coating or during the weighing process. To test this hypothesis, one AL4MG1 and AL4CA1 batch (numbers 69 and 70) were coated as soon as possible after pretreatment, without weighing or the usual one day storage in the Dri-Train. After coating, they were aged in air the usual one day and then tested. Comparison with the results obtained with the standardly prepared AL4MG1 and AL4CA1 wires indicated that oxidation of the substrate was not responsible for this unexpected trend in the data.

Other possibilites which could explain the fact that the power data for the AL4MG1 and AL4MG2 wires are higher than those for the AL4 wires are the formation of metal halides such as AlF_3 or MgF_2 due to inadequate washing in methanol after the acid etch. However, the trend to lower powers for the AL4MG3 and AL4MG4 is inconsistent with the formation of such flourides.

Thus it is felt that the trends in the total power data are due to pinholes in the coatings which result from the increased

substrate roughness after the HF etch. Such pinholes then allow formation of Al_2O_3 either during storage or during the ohmic heating period and result in high powers at breaking as for the AL2MG wires. As the number of Mg doses was increased from one to four, the probability of covering the pinholes in any given layer increased. Again the necessity of preventing Al_2O_3 formation or removing the Al_2O_3 film on the substrate when coating with Mg is emphasized.

The general improvement in the power requirement shown by the one week old AL4MG samples most likely results from alloying between the coating and substrate to give a better bond.

Results for the AL4CA wires are shown in Fig. 9. All samples exhibit the desired trend, as a result of inhibition of Al_2O_3 formation by the Ca coating. The agreement between the one day old and one week old wires indicates further that the AL4CA wires are storable due to better bonding between the coating and the rough, HF acid etched substrate.

e. Summary:

The conclusions obtained primarily on the basis of the total power required to break coated Al wires in O_2 in the wire-burning apparatus are summarized as follows:

1. 1 to 3 μ Mg coatings on CH_3OH washed (AL2) wires require greater powers than as-received (AL) wires, probably due to alloying between the MgO and pre-existing Al_2O_3 coat to form a high melting temperature spinel. These wires are storable for a least a week in NTP air.

2. Similar coatings of Ca on AL2, although oxidizing rapidly and spalling from the wire during storage, exhibit lower power requirements than AL wires. Evidently the Al oxidation is impeded by the remaining Ca or CaO coat. Samples so treated are not storable even for times as short as a week.

3. One day old amalgamated Al (AL3) wires require higher powers than AL wires due to formation of a thick Al_2O_3 coat, which may be able to self-heal. Fresh AL3 wires break more readily than AL wires, but in general AL3 processed Al cannot be stored. 100% ignition reproducibility for both types of AL3 wires indicates that the critical temperature is always exceeded during the ohmic heating period, but this conclusion has no significance other than in the wire-burning apparatus.

4. AL3MG wires exhibit the desired trend in power at breaking as the Mg coat is able to prevent Al_2O_3 formation during up to one week of storage and during heating. It is thought that 1 to 3 μ Mg coatings were applied to the samples. Comparison with the AL2MG results demonstrates that it is essential to remove the pre-existing Al_2O_3 film before coating with Mg.

5. The spalling typical of Ca coatings is accelerated if the substrate has been amalgamated, and thus the AL3CA samples are less efficient than the AL samples. These samples are not storable for times as short as one day.

6. HF etched substrates which are characterized by a high degree of surface roughness require more Mg doses to cover all pinholes and prevent Al_2O_3 formation. Otherwise, AL4MG wires behave similarly to AL2MG samples. Storing improves the performance of the AL4MG wires, probably as a result of alloying and thus better bonding between the coating and substrate.

7. Due to the roughness of the substrate, Ca coatings bond better to the AL4 substrate and not only exhibit the improvement in ignition characteristics typical of Ca coatings, but also are storable for times up to one week.

8. All of the pretreatments and coatings applied affected the ignition, but not combustion of Al wires. However, this conclusion is based only on visual observation.

To conclude, the most straightforward and promising means of improving the ignition efficiency of Al appears to be amalgamating the Al to remove any Al_2O_3 film and then coating the clean substrate with Mg. HF etching techniques are inconvenient because of the hazards of the etching solution and require a greater number of doses of the coating material. Ca coatings in general may not be compatible with solid propellant materials and thus may also present a hazard during storage.

It is felt that the general considerations from the ignition model of augmenting metal ignition efficiency have been verified insofar as possible in the wire-burning apparatus.

VI. FUTURE DEVELOPMENTS

During the next contract year, the major emphasis will shift to experimentation in the induction furnace facility to determine ignition and critical temperatures as a function of the metal-oxidizer system and surface area/volume ratio, gas composition and pressure. Mg and Al in O_2-Ar, O_2-CO_2, and CO_2-Ar atmospheres will receive the most study. Upon completion of this study, a few experiments with AL3MG samples will be performed to check the conclusions obtained in the wire-burning apparatus.

REFERENCES CITED IN THE TEXT

1T. Frank-Kamenetskii, D.A., Diffusion and Heat Exchange in Chemical Kinetics, Thon, N., translator, Princeton University Press, Princeton, 1955.

2T. Gulbransen, E.A. (1949), Ind. Eng. Chem. 41, 1385.

3T. Sleppy, W.C. (1961), J. Electrochem. Soc. 108, 1097.

4T. Alymore, D.W., Gregg, S.J., and Jepson, W.B. (1960), J. Nucl. Mater. 2, 169.

5T. Cubicciotti, D.(1950), J. Amer. Chem. Soc. 72, 2084.

6T. Kuehl, D.K. (1965), AIAA J. 3, 2239.

7T. Hodgman, C.D., editor, Handbook of Chemistry and Physics, 42nd Edition, Chemical Rubber Publishing Co., Cleveland, 1960.

8T. Alymore, D.W., Gregg, S.J., and Jepson, W.B.(1960), J. Inst. Met. 88, 205.

9T. Gulbransen, E.A. (1945), Trans. Electrochem. Soc. 87, 589.

10T. Cubicciotti, D.(1952), J. Amer. Chem. Soc. 74, 557.

11T. Kubaschewski, O., and Hopkins, B.E., Oxidation of Metals and Alloys, Second Edition, Butterworths, London, 1962.

12T. Bartlett, R.W. (1965), J. Electrochem. Soc. 112, 744.

13T. Bartlett, R.W. (1964), ML-TDR-64-290.

14T. Albrecht, W.M., Klopp, W.D., Koehl, B.G., and Jaffee, R.I. (1961), Trans. AIME 221, 110.

TABLE 1.

ESTIMATED TRANSITION TEMPERATURES

System	T_{trans}, °C	Mechanism
$Al-O_2$	2030	[b]
$Mg-O_2$	450	[e] or [f]
$Mg-CO_2$	550	[e] or [f]
$Ti-O_2$	850	[c]
$Zr-O_2$	900 ± 100	[c] or [f]
$Ta-O_2$	500	[f]
$Mo-O_2$	700	[b] or [f]
$Ca-O_2$	400	[e] or [f]
$Si-O_2$	$1400 < T_{trans} < 1610$	[b] ?
$U-O_2$	250	[d]

TABLE 2.

EXPERIMENTAL IGNITION TEMPERATURES OF MAGNESIUM

ATMOSPHERE	CONDITION	STATED SIZE	IGNITION TEMPERATURE, °C	REFERENCE
AIR	DD[1]		520	(53)
	DD	$< 40\mu$	510	(205)
	QP[2]	$< 53\mu$	478	(333)
	DD	$40 - 66\mu$	551	(205)
	DD	$< 74\mu$	520	(177)
	DD	$< 74\mu$	620	(333)
	QP	$< 74\mu$	490	(333)
	DD	$< 149\mu$	613	(178)
	QP	$< 149\mu$	517	(178)
	QP	$< 149\mu$	520	(333)
		$< 53\mu$	510	(454)
	QP	$< 44\mu$	563	(477)
OXYGEN	B[3]		649	(157)
	B	~ 10 g.	623	(28), (248)
	B		591	(339)
WATER VAPOR	B		635	(157)

[1]Dust Dispersion; [2]Quiescent Pile; [3]Bulk

TABLE 2. (Cont.)

ATMOSPHERE	CONDITION	STATED SIZE	IGNITION TEMPERATURE, °C	REFERENCE
CARBON DIOXIDE	QP	$<44\mu$	749	(323), (330)
	QP	$<53\mu$	630	(333)
	QP	$<149\mu$	630	(178)
	B		642	(261)
	B	1.23 mm^{-1}	880	(232), (251)
	B	1.23 mm^{-1}	920	(232), (251)
	QP	$<74\mu$	600	(333)
NITROGEN	QP	$<53\mu$	575	(333)
	QP	$<74\mu$	550	(333)
	QP	$<149\mu$	520	(333)
	QP	$<149\mu$	530	(178)

TABLE 3

EXPERIMENTAL IGNITION TEMPERATURES FOR TITANIUM

ATMOSPHERE	CONDITION	STATED SIZE	IGNITION TEMPERATURE, °C	REFERENCE
AIR	DD		480	(53)
	DD	$<40\mu$	401	(205)
	QP	$<44\mu$	480	(333)
	QP	$<44\mu$	470	(333)
	DD	$40-53\mu$	425	(205)
	DD	$<66\mu$	412	(205)
	QP	$<74\mu$	460	(333)
	DD	$<149\mu$	480	(178)
	QP	$<149\mu$	460	(178)
	QP	$1-5\mu$	625	(477)
OXYGEN	B	2.25 to 7.88 mm^{-1}	815	(35)
CARBON DIOXIDE	QP	$<44\mu$	900	(333)
	QP	$<44\mu$	470	(333)
	QP	$<74\mu$	680	(333)

TABLE 3. (Cont.)

ATMOSPHERE	CONDITION	STATED SIZE	IGNITION TEMPERATURE, °C	REFERENCE
CARBON DIOXIDE	QP	$< 149\mu$	680	(178)
	QP	1200 - 6000 mm^{-1}	670	(323), (330)
	QP	445 mm^{-1}	550	(244)
	B	2.25 to 7.88 mm^{-1}	1520	(35)
NITROGEN	QP	$< 44\mu$	900	(333)
	QP	$< 44\mu$	500	(333)
	QP	$< 74\mu$	900	(333)
	QP	445 mm^{-1}	760	(244)
	QP	1200 - 6000 mm^{-1}	830	(323), (330)

TABLE 4.

EXPERIMENTAL IGNITION TEMPERATURES FOR URANIUM

ATMOSPHERE	CONDITION	STATED SIZE	IGNITION TEMPERATURE, °C	REFERENCE
AIR	B		397	(23)
	B		380	(24)
	B		330	(24)
	QP	74	145	(477)
CARBON DIOXIDE	QP	$< 74 \mu$	235	(323), (330)
	DD	556 mm^{-1}	560	(244)
	QP	556 mm^{-1}	350	(244)
	B	.9 mm^{-1}	800	(251)
NITROGEN	QP	$< 74 \mu$	357	(323), (330)
	QP	556 mm^{-1}	410	(244)
OXYGEN			300	(435)

TABLE 5.

EXPERIMENTAL IGNITION TEMPERATURES FOR CALCIUM

ATMOSPHERE	CONDITION	STATED SIZE	IGNITION TEMPERATURE, °C	REFERENCE
AIR	B	.227-.25 mm^{-1}	730	(2)
	QP	$<44\mu$	229	(477)
OXYGEN	B	~ 10 g.	550	(28), (248)
	B		550	(36)
CARBON DIOXIDE	QP	$<44\mu$	293	(323), (330)
NITROGEN	QP	$<44\mu$	327	(323), (330)
	QP	$<44\mu$	360	(323), (330)
	QP	$<44\mu$	671	(323), (330)

TABLE 6.

EXPERIMENTAL IGNITION TEMPERATURES FOR TANTALUM

ATMOSPHERE	CONDITION	STATED SIZE	IGNITION TEMPERATURE, °C	REFERENCE
AIR	DD	$\angle 44\mu$	630	(333)
	QP	$\angle 44\mu$	300	(333)
	B	$4.32\ mm^{-1}$	1260*	(2)
OXYGEN	B	$.845\ mm^{-1}$	1300	(384)
	B	$4.2\ mm^{-1}$	1000	(123), (465)

*Brightness temperature

TABLE 7.

EXPERIMENTAL IGNITION TEMPERATURES FOR MOLYBDENUM

ATMOSPHERE	CONDITION	STATED SIZE	IGNITION TEMPERATURE, °C	REFERENCE
AIR	DD	$\angle 74\mu$	720	(333)
	QP	$\angle 74\mu$	360	(333)
OXYGEN	B	$\sim 10g.$	750	(28), (248)
	B		725	(339)
	B	$2.33\ mm^{-1}$	750	(221)

TABLE 8.

EXPERIMENTAL IGNITION TEMPERATURES FOR ZIRCONIUM

ATMOSPHERE	CONDITION	STATED SIZE	IGNITION TEMPERATURE, °C	REFERENCE
AIR	DD		25	(53)
	QP	$< 44\mu$	210	(333)
	DD	$< 149\mu$	25	(178)
	QP	$< 149\mu$	210	(178)
OXYGEN	B	15.05 mm^{-1}	820	(306)
	B	1.41 mm^{-1}	1000	(269)
			800	(386)
CARBON DIOXIDE	QP	$< 44\mu$	560	(333)
	QP	$< 149\mu$	560	(178)
	QP	2000 mm^{-1}	365	(323), (330)
	QP	2000 mm^{-1}	620	(244), (333)
	DD	1820 mm^{-1}	650	(244)
	QP	330 mm^{-1}	710	(244), (333)
NITROGEN	QP	$< 44\mu$	530	(333)
	QP	$< 149\mu$	530	(178)
	QP	2000 mm^{-1}	508	(323), (330)
	QP	2000 mm^{-1}	790	(244), (333)

TABLE 9.

EXPERIMENTAL IGNITION TEMPERATURES FOR ALUMINUM

ATMOSPHERE	CONDITION	STATED SIZE	IGNITION TEMPERATURE, °C	REFERENCE
AIR	DD		645	(53)
	DD	<44 μ	650	(333)
	QP	<44 μ	760	(333)
	QP	<44 μ	900	(333)
	DD	<74 μ	645	(177)
	QP	<74 μ	490	(333)
	DD	<149 μ	673	(178)
	QP	<149 μ	585	(178)
	QP	300,000 mm^{-1}	538	(477)
OXYGEN	DD	0-44 μ	663	(577)
	QP	3-200 μ	590	(576)
	B	7.8 mm^{-1}	2030	(326), (332), (493)
CARBON DIOXIDE	QP	<44 μ	900	(333)
	QP	<74 μ	540	(333)
	QP	<149 μ	655	(178)
	QP	706 mm^{-1}	390	(323), (330)
	QP	200,000 mm^{-1}	390	(323), (330)
	DD	44-60 μ	1600	(577)
	QP	3-200 μ	1030	(576)
WATER VAPOR	DD		NONE	(577)
	QP	3-200 μ	1130	(576)

TABLE 9. (Cont.)

ATMOSPHERE	CONDITION	STATED SIZE	IGNITION TEMPERATURE, °C	REFERENCE
NITROGEN	QP	$<44\mu$	750	(333)
	QP	$<74\mu$	800	(333)
	QP	$<149\mu$	725	(178)
MISCELLANEOUS:				
CO_2-N_2-H_2O	SP[4]	171 mm^{-1}	2030	(38)
CO_2-N_2	SP	171 mm^{-1}	2030	(39)
CO	DD		>1600	(577)
CO	QP	$3-200\mu$	740	(576)
NO	DD	$60-84\mu$	1350	(577)
NO	QP	$3-200\mu$	1060	(576)
SO_2	QP	$3-200\mu$	610	(576)
Cl_2	QP	$3-200\mu$	200	(576)
CO-Air Flame	DD		820	(577)

TABLE 10.

EXPERIMENTAL IGNITION TEMPERATURES FOR SILICON

ATMOSPHERE	CONDITION	STATED SIZE	IGNITION TEMPERATURE, °C	REFERENCE
AIR	QP	$<53\mu$	950	(333)
	QP	$<74\mu$	790	(333)

[4]Single particle

TABLE 10. (Cont.)

ATMOSPHERE	CONDITION	STATED SIZE	IGNITION TEMPERATURE, °C	REFERENCE
	QP	<149μ	950	(178)
	DD	<149μ	775	(178)
CARBON DIOXIDE	QP	< 53μ	1000	(333)
	QP	<149μ	1000	(178)
NITROGEN	QP	< 53μ	1000	(333)
	QP	<149μ	1000	(178)

TABLE 11.

EXPERIMENTAL IGNITION TEMPERATURES FOR LITHIUM

ATMOSPHERE	CONDITION	STATED SIZED	IGNITION TEMPERATURE, °C	REFERENCE
OXYGEN	B	~10 g.	190	(28), (248)
CARBON DIOXIDE	QP	<100μ	330	(323), (330)
NITROGEN	QP	<100μ	399	(323), (330)
	QP	125-149μ	170	(535)
AIR	QP	<100μ	374	(477)

TABLE 12.

EXPERIMENTAL IGNITION TEMPERATURES FOR BERYLLIUM

ATMOSPHERE	CONDITION	STATED SIZE	IGNITION TEMPERATURE, °C	REFERENCE
AIR	DD	6000 mm^{-1}	910	(333)
	QP	6000 mm^{-1}	540	(333)
		$< 37 \mu$	635	(454)
		500-2000 μ	780	(454)
	QP	$< .1 \mu$	20	(477)
H_2O-CO_2-N_2-HCl-O_2	SP	158mm^{-1}	2377	(341)

LIST OF REFERENCES FOR EXPERIMENTAL IGNITION TEMPERATURES

(2) Reynolds, W. C. (1959), NASA TN D-182.

(6) Freeman, E. S., and Campbell, C. (1963), Trans. Farad. Soc. 59, 165.

(23) Leibowitz, L.,Baker, L. Schnizlein, J. G., Mishler, L. W., and Bingle, J. B. (1963), Nucl. Sci. Eng. 15 (4), 395.

(24) Leibowitz, L., Schnizlein, J. G., and Mishler, L.W. (1963), Nucl. Sci. Eng. 15 (4), 404.

(28) Grosse, A. V., and Conway, J. B. (1958), Ind. Eng. Chem. 50.,663.

(30) **Schnizlein**, J. G., Baker, L.,and Vogel, R. C. (1960) **ANL-RCV-SL-1781.**

(35) Dean, L. E., and Thompson, W. R. (1961), ARS Journal 31 (7), 917.

(36) Pilling, N. B., and Bedworth, R. E. (1923), J Inst. Met. 29, 529.

(38) Friedman, R., and Macek, A. (1962), Combust. Flame 6, 9.

(39) Friedman, R., and Macek, A. (1963), Ninth Symposium (International) on Combustion, 703, Academic Press, New York.

(40) Hill, P. R., Adamson, D., Foland, D. H., and Bressette, W. E. (1956), NACA RM L55L23b.

(48) Cassel, H. M., and Liebman, I. (1959), Combust. and Flame 3, 467.

(53) Hartmann, I. (1948), Ind. Eng. Chem. 40, 752.

(57) Fassell, W. M., Jr., Gulbransen, L. B., Lewis, J. R., and Hamilton, J. H. (1951), J. Metals 3, 522.

(123) Cowgill, M. G., and Stringer, J., (1960), J. Less-Common Metals, 2, 233.

(129) Loriers, J. (1952), Rev. Metall. 49, 801.

(130) Brown, C. R. (1934), The Determination of the Ignition Temperatures of Solid Materials. D. Sc. Thesis, Catholic University of America.

(157) Kubaschewski, O., and Ebert, H. (1947), Z. Metallk. 38, 232.

(173) Cassel, H. M., and Liebman, I. (1963), Combust. Flame 7, 79.

(175) Loriers, J., (1952), Comptes Rendus Acad. Sci., Paris 234, 91.

(177) Hartmann, I., and Nagy, J. (1944), Bureau of Mines Report of Investigations 3751.

(178) Hartmann, I., Nagy, J., and Brown, H.R. (1943), Bureau of Mines Report of Investigations 3722.

(205) Constantinides, G. (1952), Ann. Chim. Roma 42, 383.

(221) Simnad, M., and Spilners, A. (1955), J. Met. 7, 1011.

(231) Schnizlein, J. G., Pizzolato, P. J., Porte, H.A., Bingle, J. D., Fisher, D. F., Misnler, L.W., and Vogel, R. C. (1959), ANL 5974.

(232) Darras, R., Baque, P., and Leclercq, D. (1959), Comptes Rendus Acad. Sci., Paris 249, 1647.

(244) Hartmann, I., Nagy, J., and Jacobson, M. (1951), Bureau of Mines Report of Investigations 4835.

(248) Conway, J. B., and Kirshenbaum, M. S., Ninth Progress Report Contract N9-ONR-87301, Res. Inst. Temple Univ., January 1954.

(250) Tammann, G., and Boehme, W. (1934), Z. anorg. allge. Chem. 217, 225.

(251) Darras, R., Baque, P., and Leclercq, D. (1959), NP-9715.

(261) McIntosh, A. B., and Bagley, K. Q. (1956), J. Inst. Met. 84, 251,

(269) Hayes, E. T., and Roberson, A. H. (1949), Trans. Electrochem. Soc. 96, 142.

(306) Schnizlein, J. G., Porte, H.A., Pizzolato, P. J., Bingle, J.D., Fischer, D.F., Mishler, L.W., Martin, P., and Vogel, R.C. (1958), ANL-5924.

(323) Rhein, R. A., (1964), Fall 1964 Western States Combustion Meeting, Preprint 64-25.

(326) Kuehl, D. K. (1964), Fall 1964 Western States Combustion Meeting, Preprint 64-21.

(330) Rhein, R. A. (1964), JPL Tech. Rep. No. 32-679.

(332) Kuehl, D. K. (1965), AIAA Second Aerospace Sciences Meeting, AIAA Paper No. 65-103.

(333) Jacobson, M., Cooper, A.R., and Nagy, J. (1964), Bureau of Mines Report of Investigations 6516.

(336) Anderson, H.C. and Belz, L. H. (1953), J. Electrochem. Soc. 100, 240.

(339) Baur, J.P., Bridges, D.W., and Fassell, W.M. Jr. (1955), J. Electrochem. Soc. 102, 490.

(341) Macek, A., Friedman, R., and Semple, J. M., (1964) Heterogeneous Combustion, Wolfhard, H G., Glassman, I., and Green, L., Jr., editors, 3. Academic Press, New York.

(384) Albrecht, W.M., Klopp, W.D., Koehl, B.G., and Jaffee, R.I. (1961), Trans. AIME 221, 110.

(386) Gulbransen, E.A. and Andrew, K.F. (1958), Trans. AIME 212, 281.

(435) Leibowitz, L., Bingle, J.D., and Homa, M. (1964), J. Electrochem. Soc. 111, 248.

(454) Fairbairn, A. (1965), UKAEA AHSB(S)R80.

(465) Cowgill, M.G. and Stringer, J. (1961) Niobium, Tantalum, Molybdenum, and Tungsten, Quarrell, A.G., editor, 190. Elsevier, Amsterdam.

(475) Cassel, H.M. (1964), Bureau of Mines Report of Investigations 6551.

(477) Rhein, R.A., (1965), JPL Space Programs Summary No. 37-31, Vol. IV, 201.

(493) Kuehl, D.K., (1965), AIAA J., 3, 2239.

(535) Markowitz, M.M., and Boryta, D.A. (1962), Chem. and Eng. Data Z, 586.

(576) Smolenski, D., and Seweryniak, M. (1963), Bilv. Wojskowej. Acad. Tech. 12 (4), 43. (Chem. Abstracts 60, 1529, 1964.)

(577) Smolenski, D., and Seweryniak, M. (1963), Bivl. Wojskowej. Acad. Tech. 12 (5), 37. (Chem. Abstracts 60, 1529, 1964)

TABLE 13.

INPUT AND RESULTS OF THE ADIABATIC METAL PROBLEM

(Numbers in parentheses refer to references)

Value and Units	Clean Al in O_2	Mg on Al in O_2	Ca on Al in O_2
K, cal/cm sec$^{\circ}$K	1.01 (7T)	1.01 (7T)	1.01 (7T)
ρ, g/cm^3	2.702 (7T)	2.702 (7T)	2.702 (7T)
C_p, cal/g$^{\circ}$K	0.25 (7T)	0.25 (7T)	0.25 (7T)
K_p, (g metal)^2/cm^{4}sec	10^{-14} (8T)	10^{-15} (9T)	10^{-12} (10T)
Q, cal/g metal	7500 (7T)	5930 (7T)	3790 (7T)
T_{trans}, $^{\circ}$K	2303	723	673
T_o, $^{\circ}$K	100, 600, 1100, 1600, 2100	100, 600	100, 600
A	1.096×10^{15}	1.096×10^{16}	1.096×10^{13}
DT_o, $^{\circ}$K	30000	23720	15160
θ (at T_o=100°K)	39.0	41.4	34.2

TABLE 14.

INPUT AND RESULTS OF THE ADIABATIC PARTICLE PROBLEM

(Numbers in parentheses refer to references)

Value and Units	Clean Al in O_2	Mg on Al in O_2	Ca on Al in O_2
K_1, cal/cm sec°K	1.01 (7T)	1.01 (7T)	1.01 (7T)
K_2, cal/cm sec°K	0.0826 (7T)	0.087556 (7T)	0.087556*
ρ_1, g/cm^3	2.702 (7T)	2.702 (7T)	2.702 (7T)
ρ_2, g/cm^3	3.7 (7T)	3.58 (7T)	3.346 (7T)
c_{p1}, cal/g°K	0.25 (7T)	0.25 (7T)	0.25 (7T)
c_{p2}, cal/g°K	0.197 (7T)	0.232 (7T)	0.197 (7T)
γ	1.28 (11T)	0.81 (11T)	0.64 (11T)
K_p, (g metal)^2/cm^{4}sec	10^{-14} (8T)	10^{-15} (9T)	10^{-12} (10T)
Q, cal/g metal	7500 (7T)	5930 (7T)	3790 (7T)
T_{trans}, °K	2303	723	673
T_o, °K	100,600 1100,1600,2100	100,600	100,600
B_1	1.096×10^{15}	1.096×10^{16}	1.096×10^{13}
B_2	8.23×10^{13}	7.7×10^{14}	9.7×10^{11}
$B_3 T_o$, °K	30000	23720	15160
β_1	1.30	2.62	2.37
β_2	4.75	9.87	7.98

* K_{CaO} was assumed equal to K_{MgO}.

TABLE 15.

AVERAGED EXPERIMENTAL DATA FOR MOLYBDENUM

Reaction Regime	Initial Sample Weight, mg	Recovered Sample Weight, mg	Total Power, Watts		Total Resistance, ohms		Total Burning Time, sec
			at Ignition	at Breaking	at Ignition	at Breaking	
1 Overall	685.6	567.1	50.3	35.4	.073	.238	6.37
1 O_2-Ar	685.1	552.6	47.1	33.3	.072	.231	5.90
1 O_2-CO_2	686.6	607.5	56.5	40.4	.075	.256	7.75
2	682.2	668.5	———	287.6	———	.116	———
3	683.2	611.7	———	218.6	———	.141	———
4	685.1	676.6	———	193.3	———	.119	———
H_2O-Ar	690.0	531.3	———	335.2	———	.178	———
H_2O-CO_2	687.8	564.0	———	254.9	———	.183	———
H_2O-O_2	686.6	533.8	66.6	49.2	.076	.190	5.82

TABLE 16.

ALUMINUM SUBSTRATE PRETREATMENTS

DESIGNATION	PRETREATMENT	PRE-EXISTING Al_2O_3 Film Removed
AL	As-received	No
AL1	$\sim$ 5 min in Benzin, $<$ 1 hr outgassing	No
AL2	30 min in methanol, 1 hr outgassing	No
AL3	2 min in $HgCl_2$ sol., 15 min in methanol	Yes
AL4	1 hr in dil. HF, 15 min in methanol	Yes

TABLE 17.

EXAMPLES OF WEIGHT GAIN REPRODUCIBILITY ON INDIVIDUAL WIRES

Batch Number	Substrate Material	Coating Material	Wire Number	Initial Weight,mg	Final Weight,mg	Weight Gain,mg
24	AL2	1 dose of Ca	1	185.5	186.3	0.8
			2	185.2	186.0	0.8
			3	185.2	186.0	0.8
			4	185.4	186.3	0.9
			5	185.3	186.1	0.8
			6	185.4	186.2	0.8
			7	185.1	186.0	0.9
			8	184.9	185.6	0.7
			9	185.0	185.7	0.7
			10	186.0	186.5	0.5
			11	185.8	186.3	0.5
			12	185.7	186.3	0.6
			13	185.4	186.0	0.6
			14	185.4	186.0	0.6
			15	185.3	186.0	0.7
			16	185.8	186.4	0.6
25	AL2	1 dose of Mg	1	184.8	185.3	0.5
			2	186.2	186.6	0.4
			3	185.8	186.3	0.5
			4	185.2	185.8	0.6
			5	185.0	185.5	0.5
			6	185.3	185.8	0.5
			7	185.2	185.7	0.5
			8	184.8	185.4	0.6
			9	185.3	185.7	0.4

TABLE 17 (Cont'd)

Batch Number	Substrate Material	Coating Material	Wire Number	Initial Weight, mg	Final Weight, mg	Weight Gain, mg
			10	185.8	186.3	0.5
			11	185.0	185.5	0.5
			12	185.7	186.2	0.5
			13	185.2	185.8	0.6
			14	185.5	186.1	0.6
			15	185.2	185.7	0.5
			16	186.1	186.5	0.4

TABLE 18.

AVERAGE WEIGHT GAIN DATA FOR BATCHES USED IN BREAKING POWER AVERAGES (AL2 WIRES)

Average Representation	Batches Used in Average Breaking Power Calculation	Average Weight Gain Per Wire, mg
AL2MG1	25	0.5
	28	0.6
AL2MG2	16	1.6
	26	1.3
AL2MG3	18	2.4
	27	2.3
AL2CA1	17	1.0
	24	1.1
AL2CA2	30	1.2
	32	0.0
	35	2.1
AL2CA3	33	2.8
	36	3.2
AL2CA1 (fresh)	29	1.0
	34	1.0
AL2MG1 (one week old)	22	0.9
AL2CA1 (one week old)	23	1.2
AL2MG2 (one week old)	40	1.6
AL2CA2 (one week old)	38	0.4
AL2MG3 (one week old)	39	1.9
AL2CA3 (one week old)	37	0.2

TABLE 19.

AVERAGE WEIGHT GAIN DATA FOR BATCHES USED IN BREAKING POWER AVERAGES (AL3 WIRES)

Average Representation	Batches Used in Average Breaking Power Calculation	Average Weight Gain Per Wire, mg
AL3MG1	41	0.0
	47	-1.6
AL3MG2	44	0.4
	49	0.4
AL3MG 3	45	-7.0
	52	1.6
AL3CA1	42	-2.6
	48	-2.9
AL3CA2	43	0.2
	50	1.5
AL3CA3	46	-3.4
	53	-5.0
AL3MG1 (one week old)	55	-5.4
AL3CA1 (one week old)	56	-7.8
AL3MG2 (one week old)	57	-0.8
AL3CA2 (one week old)	58	0.4
AL3MG3 (one week old)	59	0.1
AL3 CA3 (one week old)	60	-1.1

TABLE 20.

AVERAGE WEIGHT GAIN DATA FOR BATCHES USED IN BREAKING POWER AVERAGES (AL4 WIRES)

Average Representation	Batches Used in Average Breaking Power Calculation	Average Weight Gain Per Wire, mg
AL4MG1	61	0.0
	69	---*
AL4MG2	63	1.3
	71	0.9
AL4MG3	65	1.7
	75	2.7
AL4MG4	85	2.3
AL4CA1	62	0.8
	70	--- *
AL4CA2	64	0.9
	72	0.8
AL4CA3	66	1.9
	76	2.4
AL4MG1 (one week old)	79	-0.2
AL4CA1 (one week old)	80	0.1
AL4MG2 (one week old)	81	1.0
AL4CA2 (one week old	82	1.4
AL4MG3 (one week old)	83	1.7
AL4CA3 (one week old)	84	4.0

*No weighings were performed on batches 69 and 70.

TABLE 21.

EFFECT OF AGING: AVERAGED WIRE WEIGHT AS A FUNCTION OF TIME AFTER COATING (AL2 WIRES)

Batch Number	Batch Representation	Average Initial Weight, mg	Average Final Weight, mg, after				
			0 days	1 day	2 days	4 days	7 days*
22	AL2MG1	184.7	185.7	185.5	185.7	185.7	185.7
23	AL2CA1	184.8	185.8	186.2	186.2	186.2	186.0
40	AL2MG2	185.1	186.6	186.5	186.5	186.6	186.7
38	AL2CA2	185.2	187.1	186.6	185.8	185.7	185.6
39	AL2MG3	185.2	187.1	187.0	187.0	187.1	187.1
37	AL2CA3	185.2	188.0	188.2	186.1	185.8	185.4

*All batches were outgassed for 65.5 hr between the 4th and 7th day readings.

TABLE 22.

EFFECT OF AGING: AVERAGED WIRE WEIGHT AS A FUNCTION OF TIME AFTER COATING (AL3 WIRES)

Batch Number	Batch Representation	Average Initial Weight, mg	Average Final Weight, mg, after				
			0 days	1 day	2 days	4 days	7 days*
55	AL3MG1	188.4	184.0	184.1	184.1	183.5	183.4
56	AL3CA1	190.1	182.2	183.2	183.0	182.6	182.3
57	AL3MG2	182.7	182.1	182.1	182.0	182.0	181.9
58	AL3CA2	185.1	186.6	186.4	185.8	185.5	185.5
59	AL3MG3	184.0	184.2	184.6	184.5	184.1	184.1
60	AL3CA3	185.6	187.5	185.8	184.8	184.6	184.5

*All batches were outgassed for 65.5 hr between the 4th and 7th day readings.

TABLE 23.

EFFECT OF AGING: AVERAGED WIRE WEIGHT AS A FUNCTION OF TIME AFTER COATING (AL4 WIRES)

Batch Number	Batch Representation	Average Initial Weight, mg	Average Final Weight, mg, after				
			0 days	1 day	2 days	4 days	7 days*
79	AL4MG1	114.4	114.3	114.3	114.2	114.2	114.2**
80	AL4CA1	118.5	118.3	118.7	118.7	118.6	118.6**
81	AL4MG2	160.4	161.4	161.3	161.3	161.3	161.4
82	AL4CA2	161.8	162.6	163.3	163.3	163.3	163.2
83	AL4MG3	167.4	169.2	169.1	169.1	169.1	169.1
84	AL4CA3	169.8	172.0	174.0	173.9	173.8	173.8

*All batches were outgassed for 65.5 hr between the 4th and 7th day readings.

**Batches #79 and #80 were inadvertantly given only 58.5 hr of outgassing.

TABLE 24.

OCCURRENCE OF GAS-PHASE SPARKS AND IGNITION

REPRODUCIBILITY (AL2 WIRES)

Batch Representation	Total Number of Runs	Number of Runs With Sparks Observed	Number of Ignitions
AL	21	0	5
AL2	21	0	11
AL2MG1	14	8	8
AL2MG2	21	14	11
AL2MG3	14	9	4
AL2CA1	14	1	5
AL2CA2	21	0	8
AL2CA3	14	1	7
AL2CA1 (fresh)	14	12	7
AL2MG1 (one week old)	7	4	4
AL2CA1 (one week old)	7	0	3
AL2MG2 (one week old)	7	3	3
AL2CA2 (one week old)	7	0	2
AL2MG3 (one week old)	7	5	3
AL2CA3 (one week old)	7	0	0

TABLE 25.

OCCURRENCE OF GAS-PHASE SPARKS AND IGNITION

REPRODUCIBILITY (AL3 WIRES)

Batch Representation	Total Number of Runs	Number of Runs With Sparks Observed	Number of Ignitions
AL	21	0	5
AL3 (fresh)	14	1	14
AL3	12	0	12
AL3MG1	14	9	5
AL3MG2	14	12	3
AL3MG3	14	11	3
AL3CA1	13	0	8
AL3CA2	14	0	2
AL3CA3	14	0	12
AL3MG1 (one week old)	7	2	1
AL3CA1 (one week old)	7	0	1
AL3MG2 (one week old)	7	0	2
AL3CA2 (one week old)	7	0	3
AL3MG3 (one week old)	7	0	0
AL3CA3 (one week old)	7	0	2

TABLE 26.

OCCURRENCE OF GAS-PHASE SPARKS AND IGNITION

REPRODUCIBILITY (AL4 WIRES)

Batch Representation	Total Number of Runs	Number of Runs With Sparks Observed	Number of Ignitions
AL	21	0	5
AL4 (fresh)	14	0	12
AL4	14	0	11
AL4MG1	14	1	7
AL4MG2	14	2	8
AL4MG3	14	5	7
AL4MG4	7	3	3
AL4CA1	14	1	4
AL4CA2	14	0	4
AL4CA3	14	4	6
AL4MG1 (one week old)	7	0	2
AL4CA1 (one week old)	7	0	0
AL4 MG2(one week old)	7	0	3
AL4CA2 (one week old)	7	0	3
AL4MG3 (one week old)	7	2	2
AL4CA3 (one week old)	7	1	1

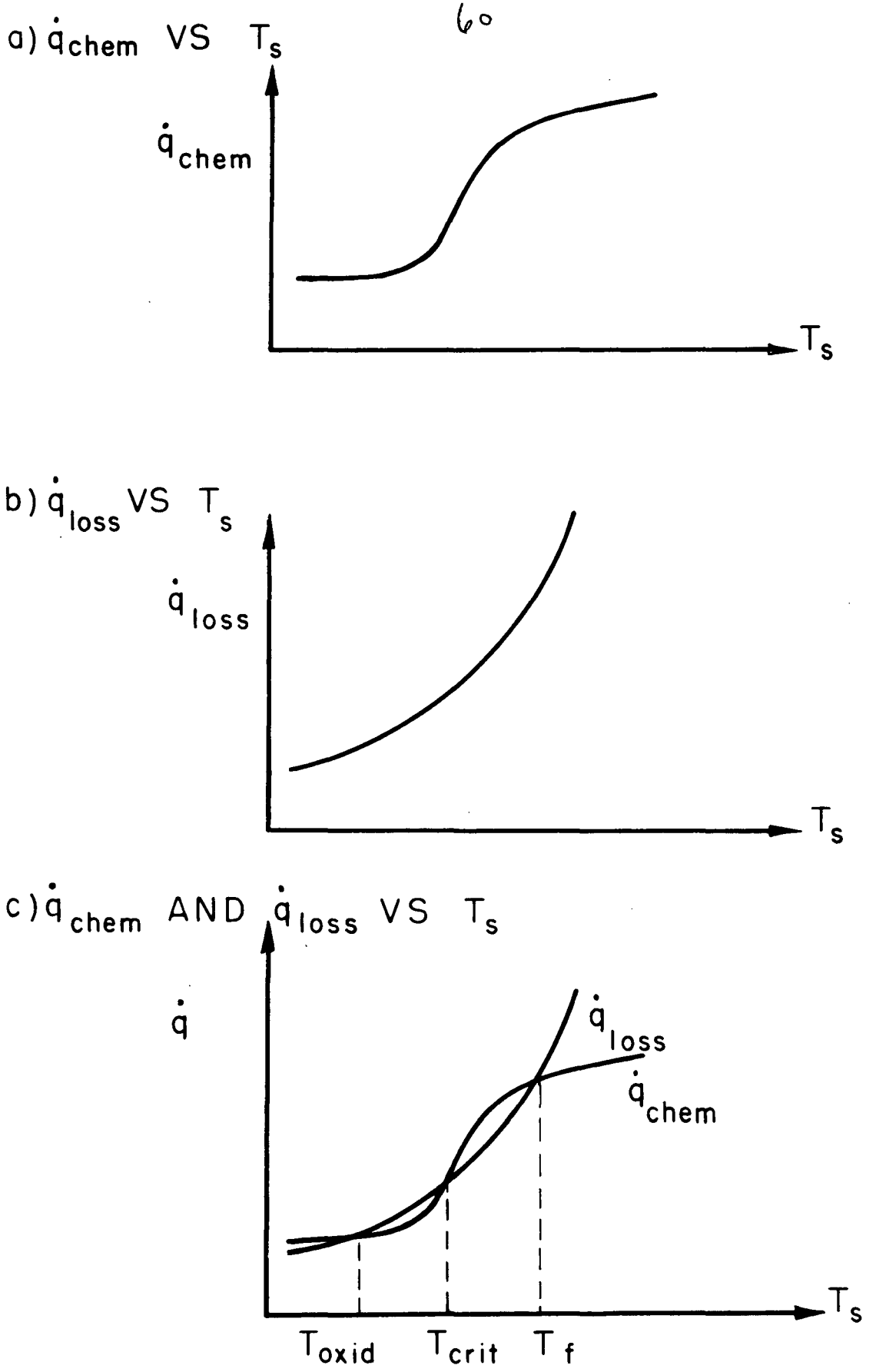

RATE OF CHEMICAL ENERGY RELEASE AND RATE OF HEAT LOSS VS SURFACE TEMPERATURE

FIGURE 1

AP29-4016-66

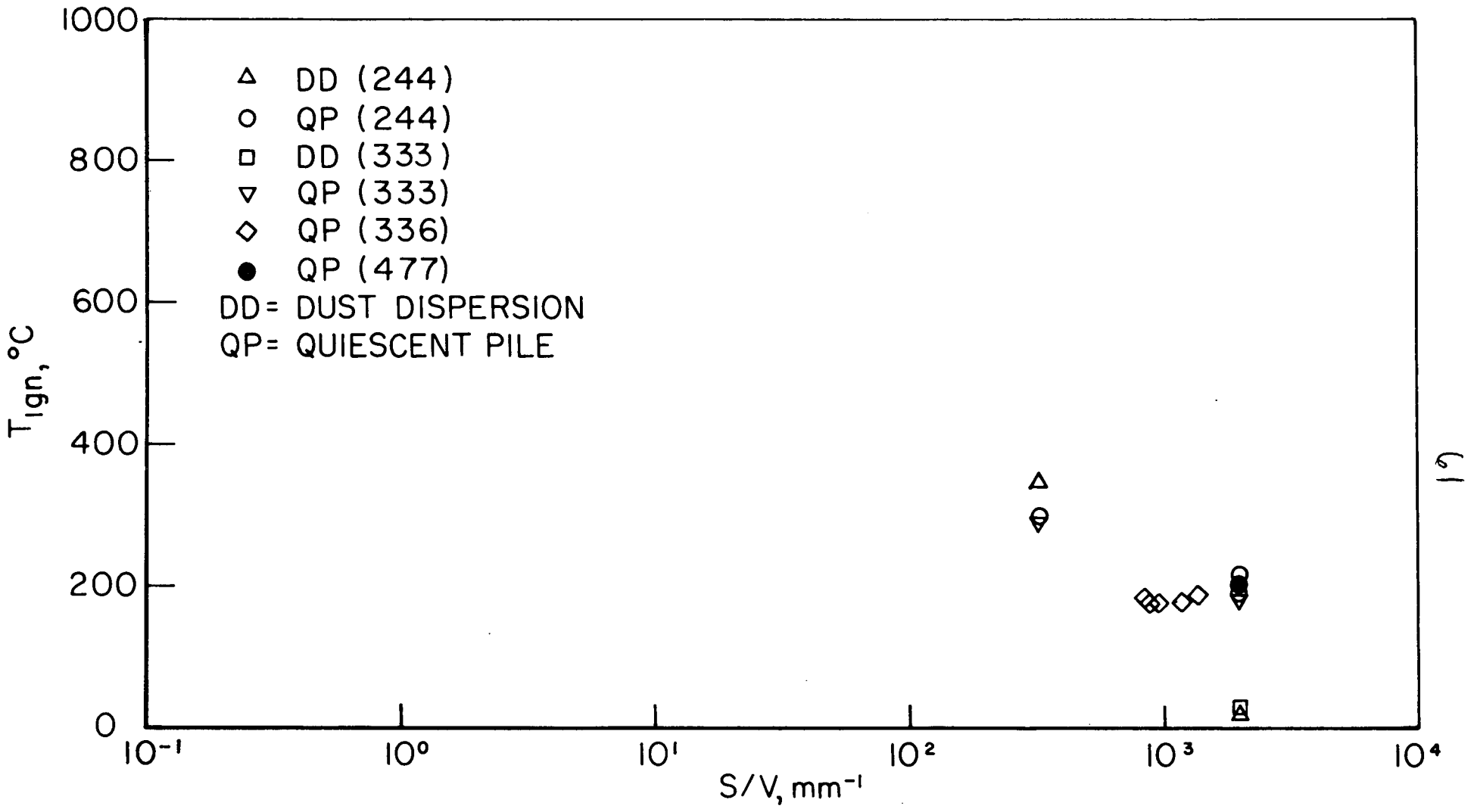

FIGURE 2

IGNITION TEMPERATURE VS SURFACE-VOLUME RATIO: ZIRCONIUM IN AIR

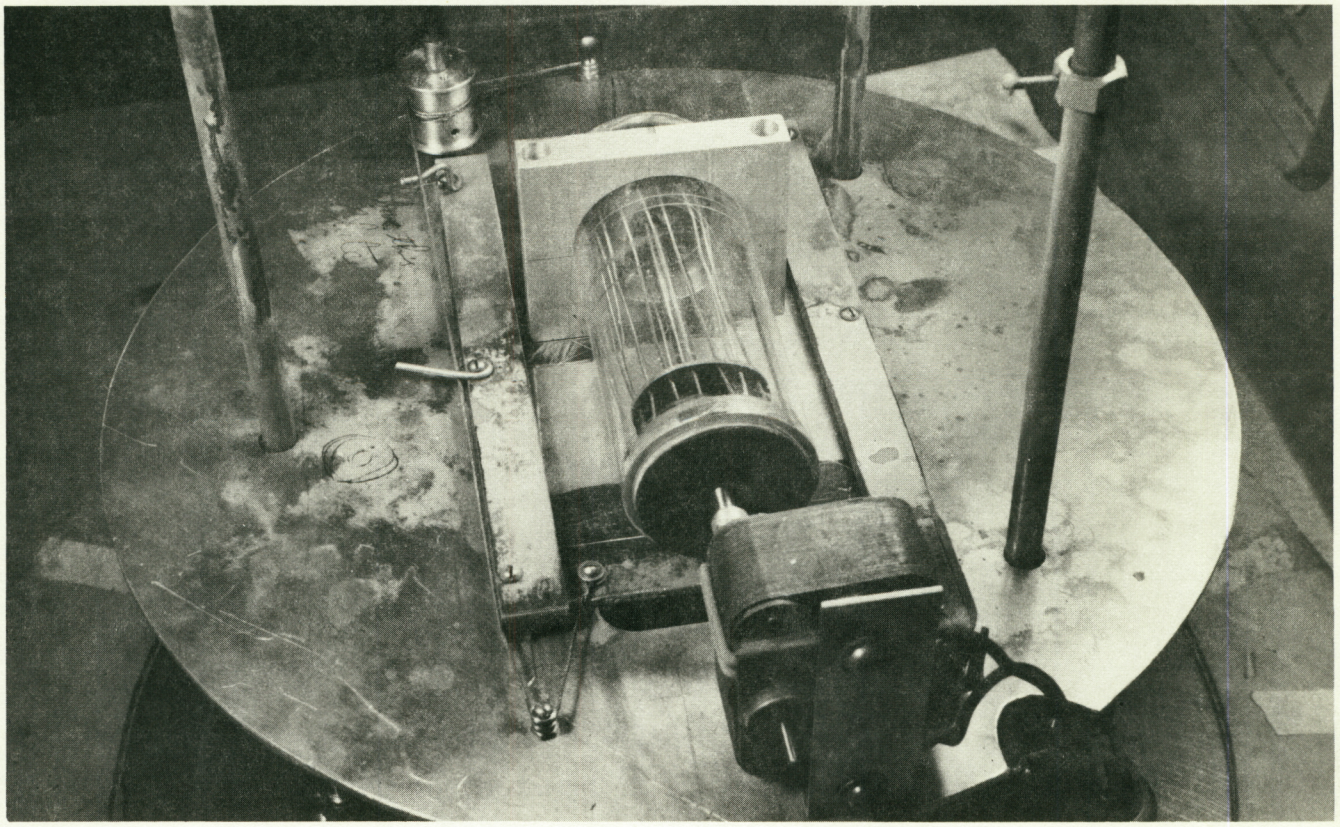

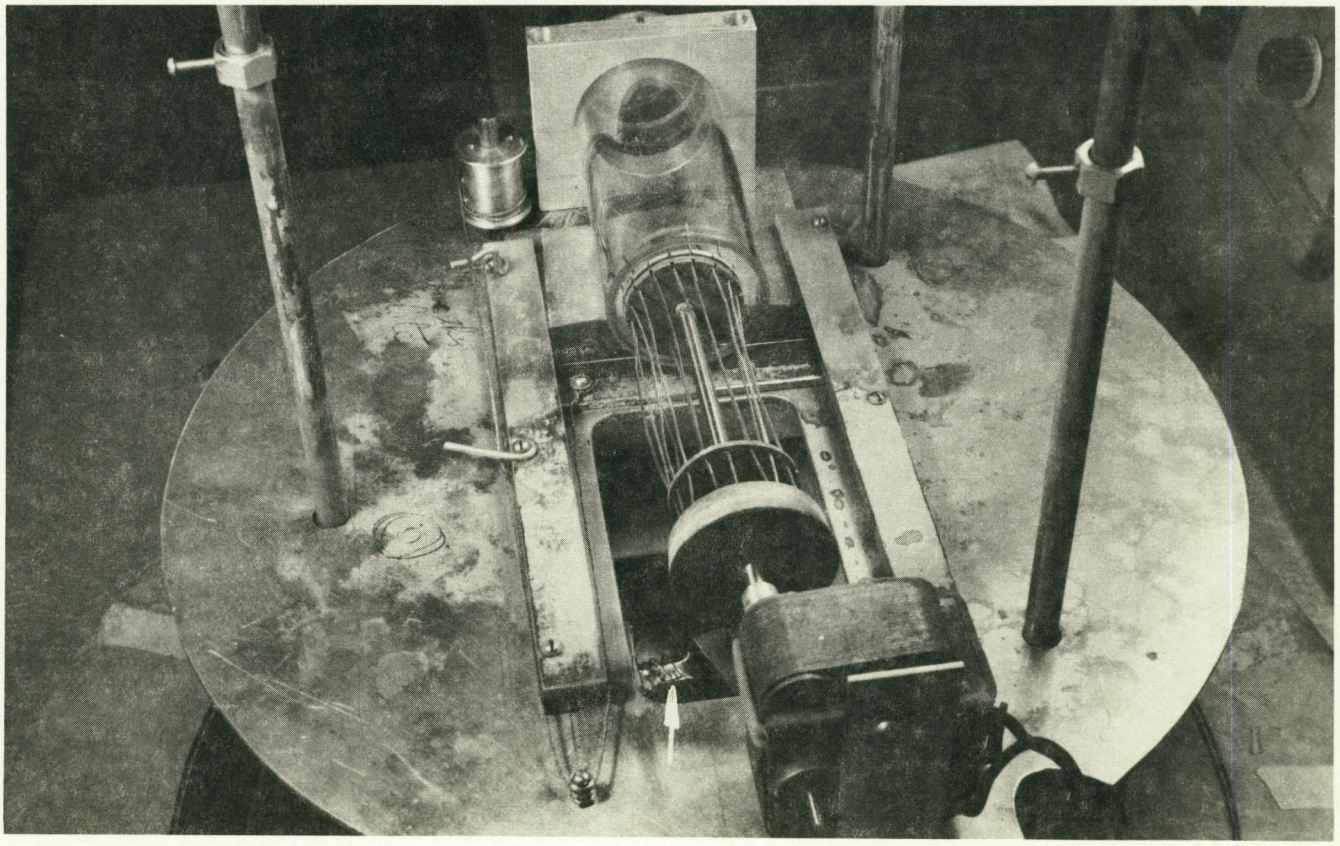

AP29-P19-66

FIGURE 3

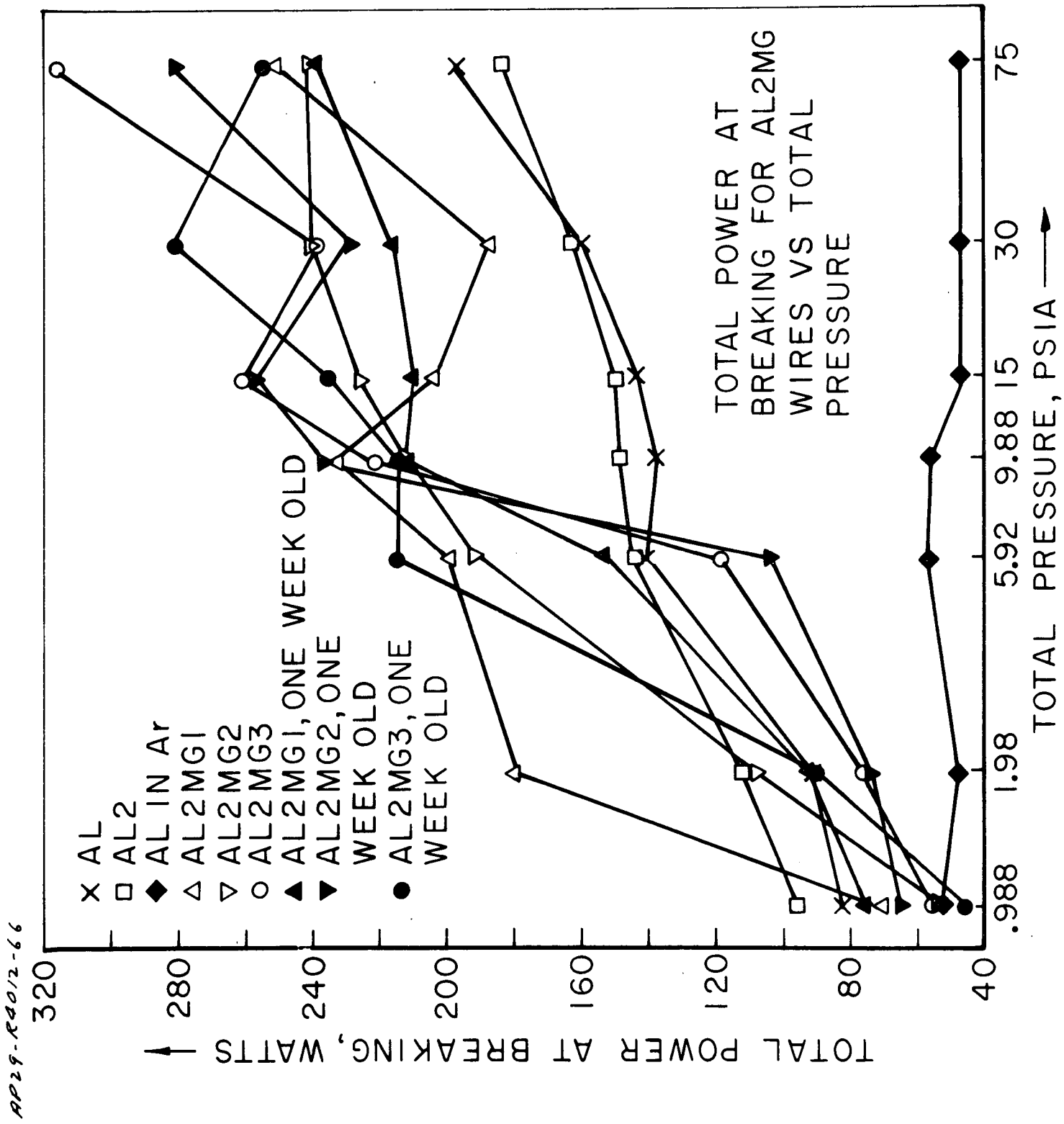
TOTAL POWER AT BREAKING FOR AL2MG WIRES VS TOTAL PRESSURE
TOTAL POWER AT BREAKING, WATTS
TOTAL PRESSURE, PSIA
320
280
240
200
160
120
80
40
.988
1.98
5.92
9.88
15
30
75
AL
AL2
AL IN Ar
AL2MG1
AL2MG2
AL2MG3
AL2MG1, ONE WEEK OLD
AL2MG2, ONE WEEK OLD
AL2MG3, ONE WEEK OLD
AP29-R40/2-66

FIGURE 4

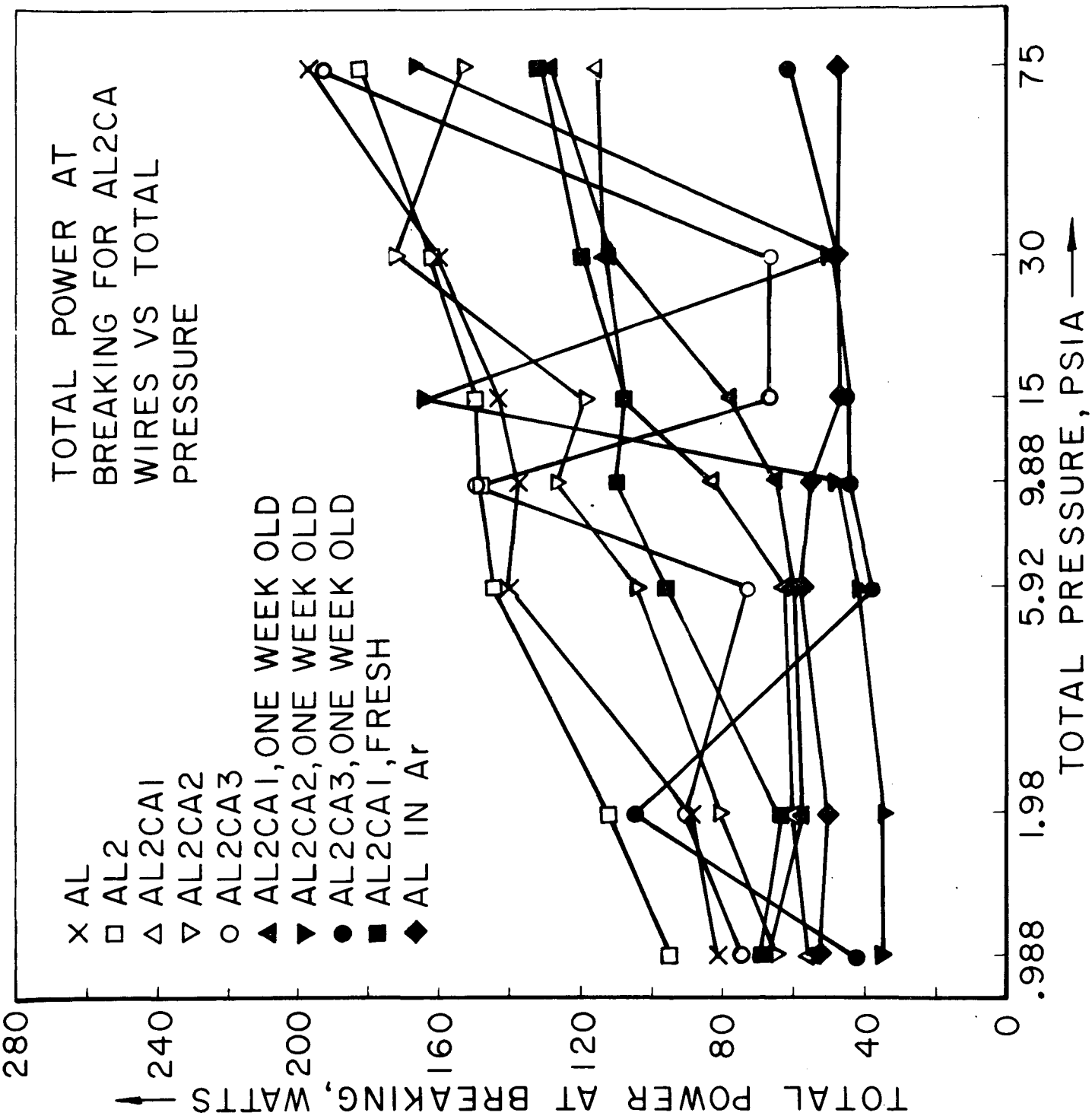

AP29-R4011-66

FIGURE 5

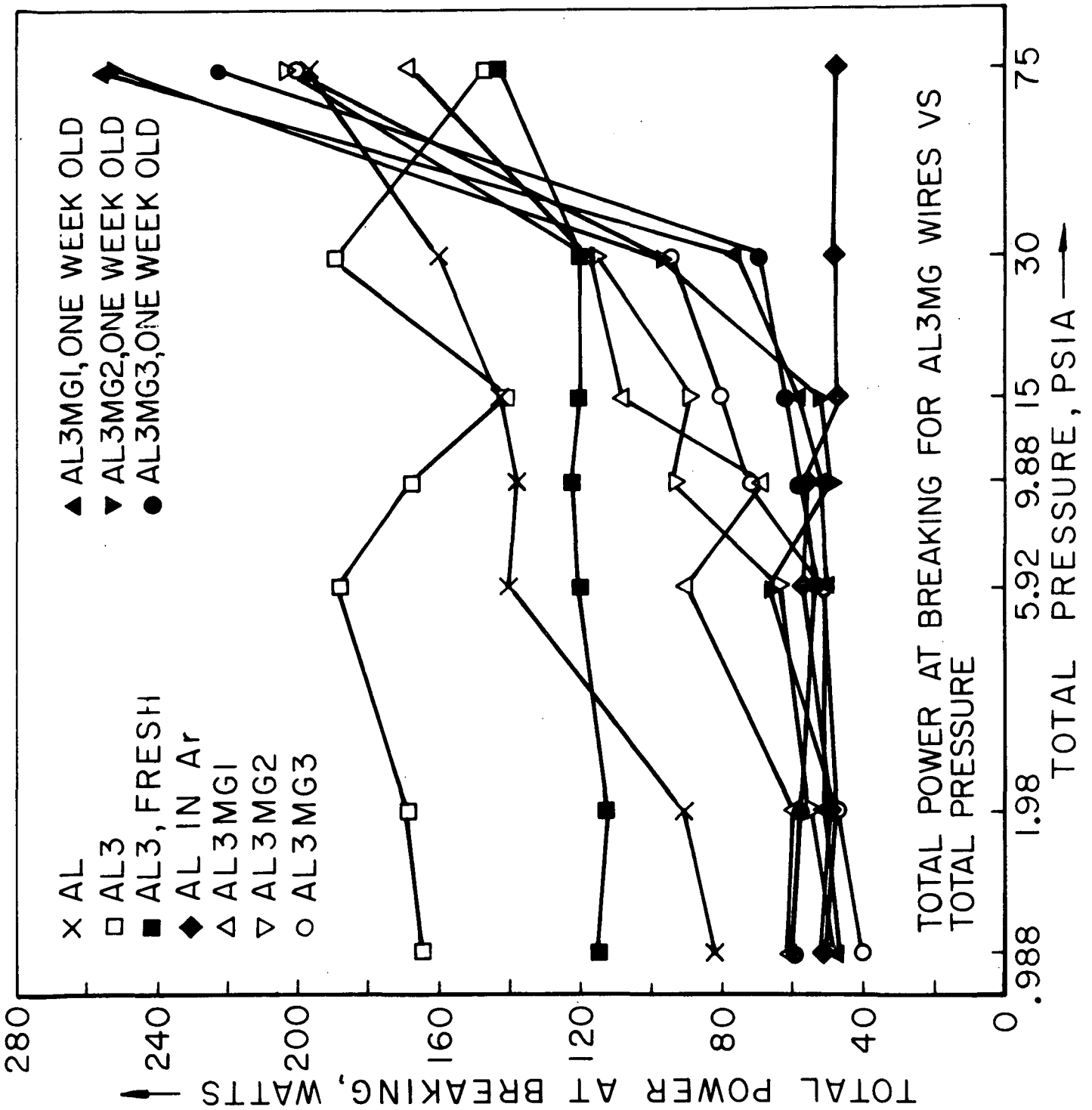

AP29-R4010-66

FIGURE 6

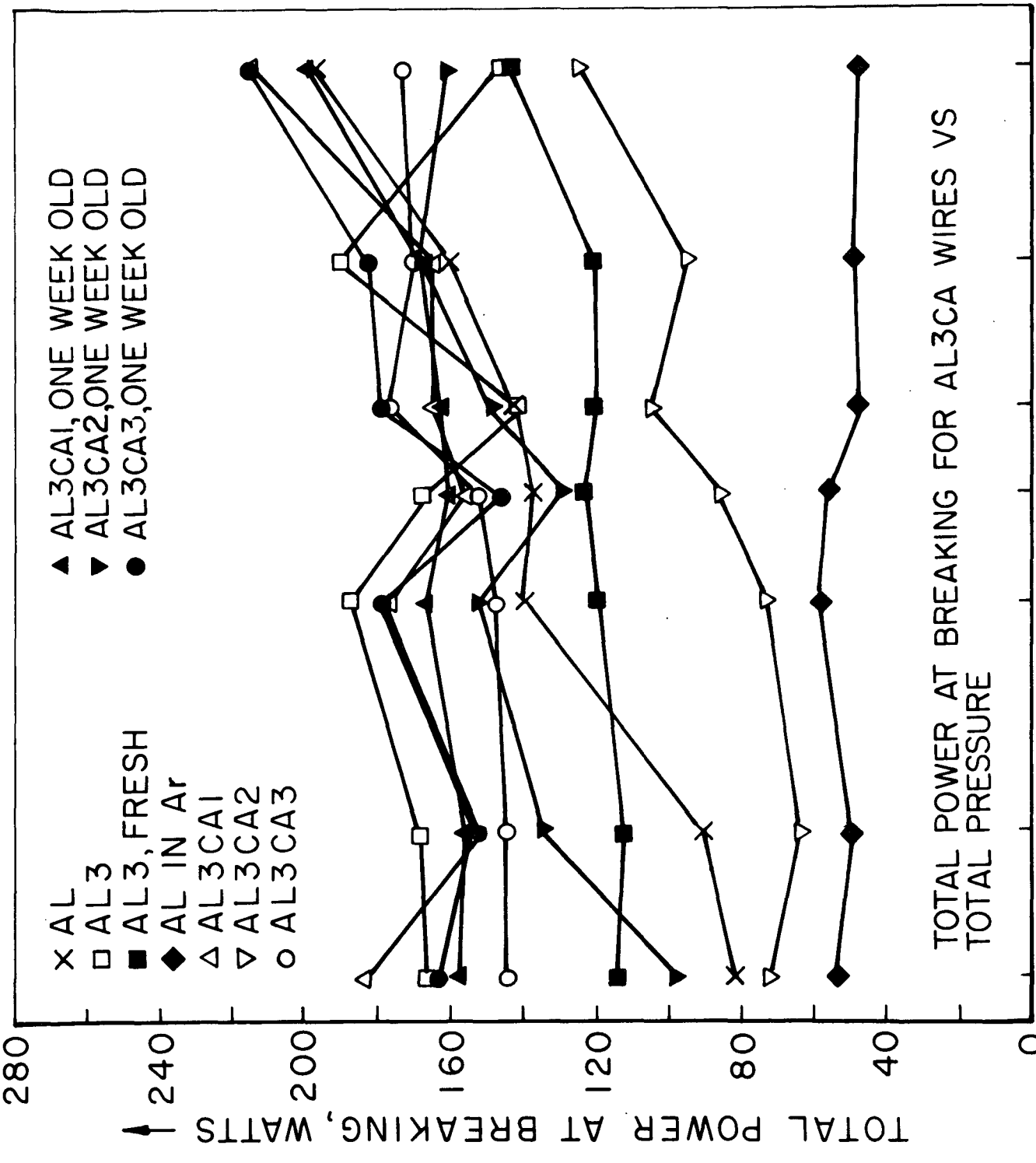
TOTAL POWER AT BREAKING, WATTS
280
240
200
160
120
80
40
0
.988
1.98
5.92
9.88
15
30
75
TOTAL PRESSURE, PSIA
TOTAL POWER AT BREAKING FOR AL3CA WIRES VS TOTAL PRESSURE
AL
AL3
AL3, FRESH
AL IN Ar
AL3CA1
AL3CA2
AL3CA3
AL3CA1, ONE WEEK OLD
AL3CA2, ONE WEEK OLD
AL3CA3, ONE WEEK OLD

FIGURE 7

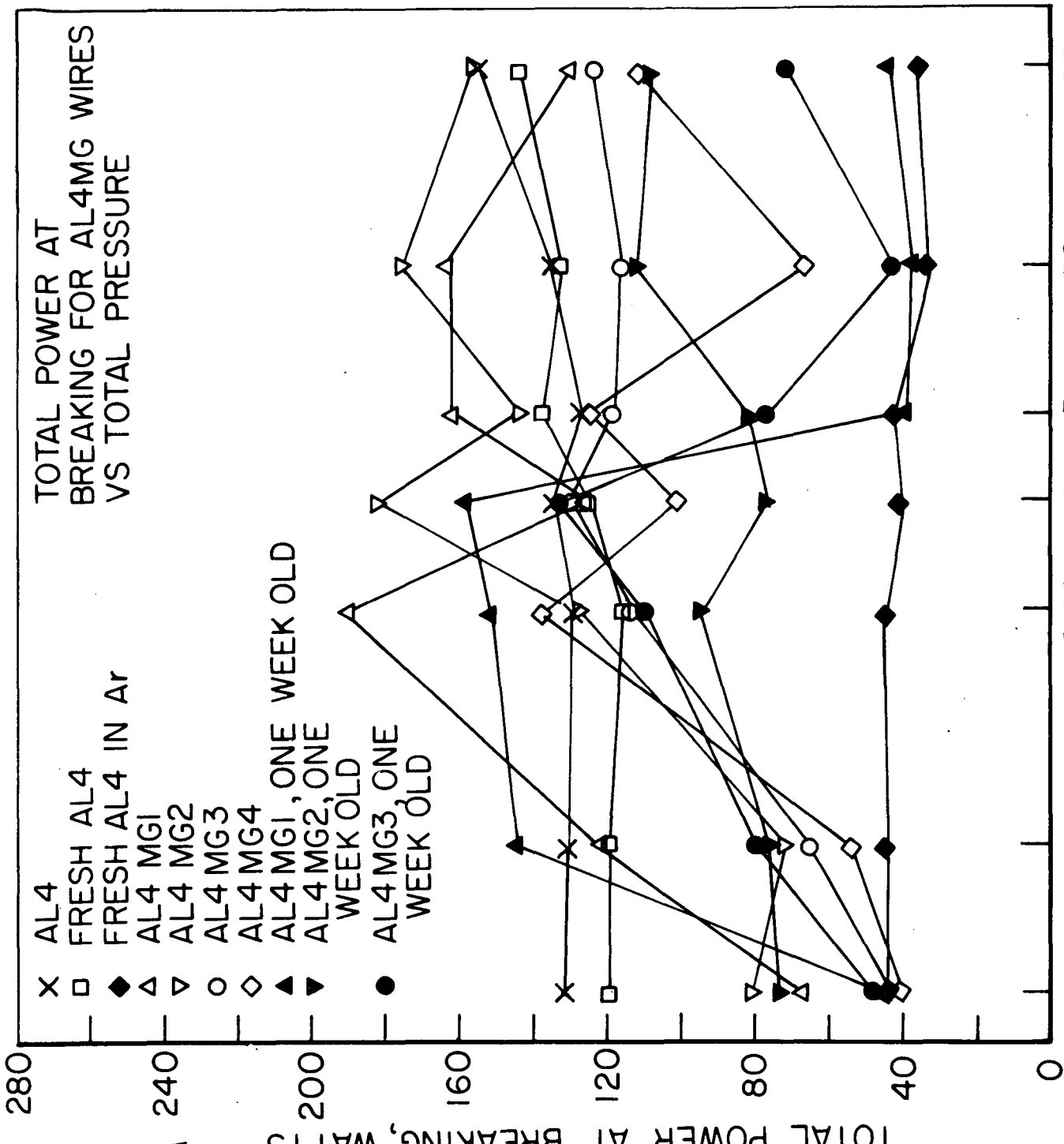

AP 29-4015-66

FIGURE 8

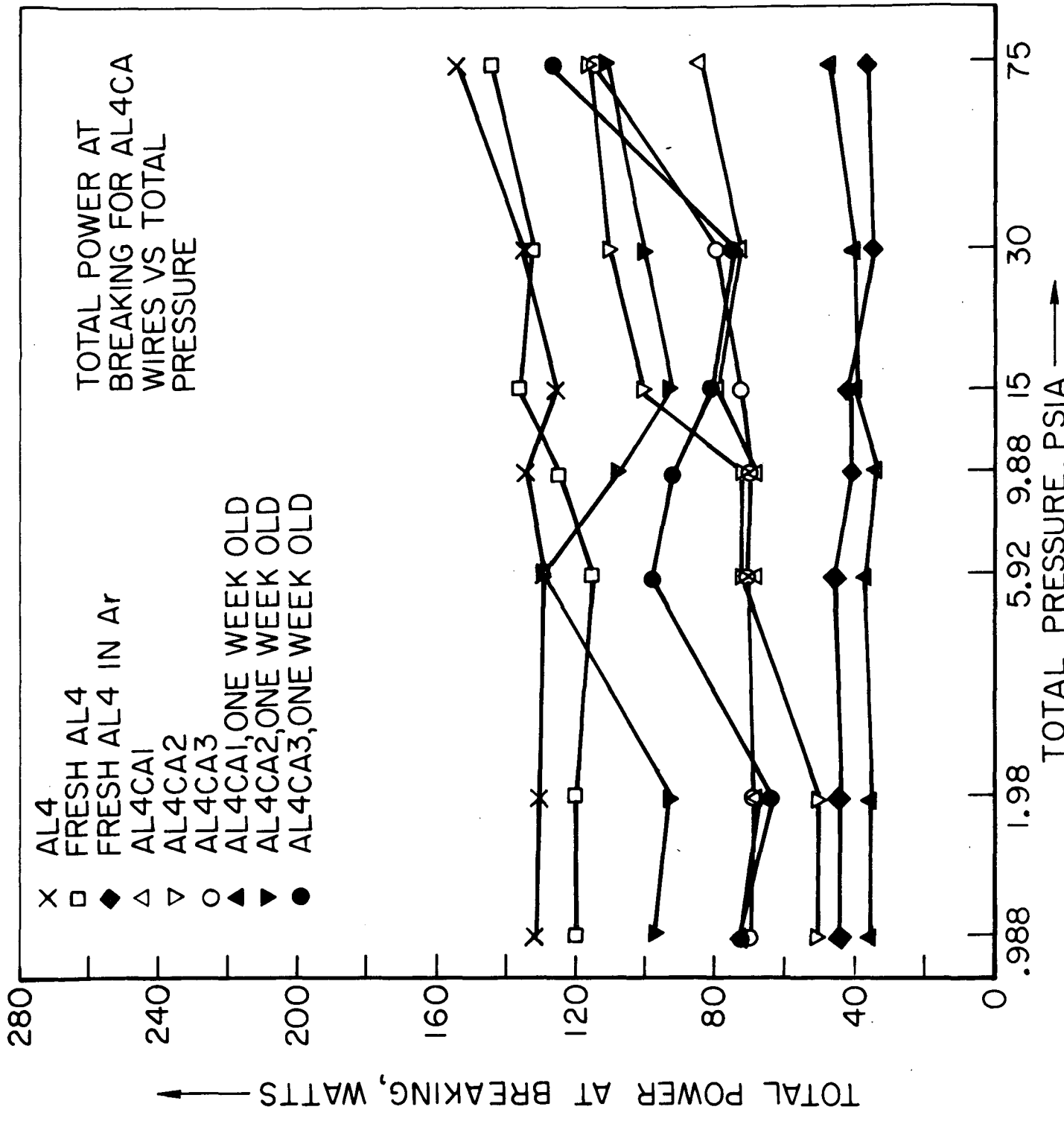

AP29-4014-66

FIGURE 9